ARTICLE

Chronic interleukin-1 exposure triggers selection for *Cebpa*-knockout multipotent hematopoietic progenitors

Kelly C. Higa[1,2,3], Andrew Goodspeed[4,5], James S. Chavez[6], Marco De Dominici[1], Etienne Danis[4,5], Vadym Zaberezhnyy[1], Jennifer L. Rabe[6], Daniel G. Tenen[7,8], Eric M. Pietras[2,5,6a], and James DeGregori[1,2,5,6b]

The early events that drive myeloid oncogenesis are not well understood. Most studies focus on the cell-intrinsic genetic changes and how they impact cell fate decisions. We consider how chronic exposure to the proinflammatory cytokine, interleukin-1β (IL-1β), impacts *Cebpa*-knockout hematopoietic stem and progenitor cells (HSPCs) in competitive settings. Surprisingly, we found that *Cebpa* loss did not confer a hematopoietic cell–intrinsic competitive advantage; rather chronic IL-1β exposure engendered potent selection for *Cebpa* loss. Chronic IL-1β augments myeloid lineage output by activating differentiation and repressing stem cell gene expression programs in a *Cebpa*-dependent manner. As a result, *Cebpa*-knockout HSPCs are resistant to the prodifferentiative effects of chronic IL-1β, and competitively expand. We further show that ectopic *CEBPA* expression reduces the fitness of established human acute myeloid leukemias, coinciding with increased differentiation. These findings have important implications for the earliest events that drive hematologic disorders, suggesting that chronic inflammation could be an important driver of leukemogenesis and a potential target for intervention.

Introduction

Hematologic disorders such as clonal hematopoiesis, myelodysplastic syndrome (MDS), myeloproliferative neoplasm (MPN), and acute myeloid leukemia (AML) are thought to originate from multipotent hematopoietic stem and progenitor cells (HSPCs), which are responsible for lifelong regeneration of the blood system. Understanding the earliest events that drive these disorders is thus important to understand the etiology of the malignancy and to devise potential intervention strategies.

Risk factors associated with hematologic disorders include age and prior exposure to radiation or chemotherapy, conditions characterized by underlying inflammation (Bowman et al., 2018). Prior studies have shown that aging, radiation, chronic infection, and chronic inflammation promote HSPC differentiation at the expense of self-renewal (Fleenor et al., 2015a; Matatall et al., 2016; Mejia-Ramirez and Florian, 2020; Pietras, 2017). The proinflammatory cytokine IL-1 is important in regulating hematopoiesis and the immune response in the acute setting, such as by promoting emergency granulopoiesis in response to infection, but can

drive pathology in the chronic setting (Mantovani et al., 2019). For instance, IL-1 can promote AML expansion in ex vivo culture (Carey et al., 2017), and increased expression of IL-1 receptor accessory protein is associated with poor prognosis in AML (Barreyro et al., 2012).

Many oncogenic mutations associated with AML are known to block differentiation and/or enhance self-renewal (Corces et al., 2017; Kelly and Gilliland, 2002; Ley et al., 2013). CCAAT/enhancer-binding protein α (C/EBPα) is a bZIP transcription factor that regulates myeloid lineage commitment in HSPCs. Its function is frequently altered in MDS/MPN and AML by loss-of-function (LOF) mutations or by (epi)genetic alterations that suppress *CEBPA* expression, such as mutations in *NPM1* or *RUNX1*, *FLT3-ITD*, *AML1-ETO*, or *BCR-ABL*, together accounting for ~70% of molecular alterations in de novo AML (Ernst et al., 2010; Gu et al., 2018; Guo et al., 2012; Ley et al., 2013; Pabst et al., 2001a; Perrotti et al., 2002; Zheng et al., 2004). Further, *Cebpa* LOF leads to a block in myeloid differentiation, contributing to

....

[1]Department of Biochemistry and Molecular Genetics, University of Colorado Anschutz Medical Campus, Aurora, CO;   [2]Integrated Department of Immunology, University of Colorado Anschutz Medical Campus, Aurora, CO;   [3]Medical Scientist Training Program, University of Colorado Anschutz Medical Campus, Aurora, CO;   [4]Department of Pharmacology, University of Colorado Anschutz Medical Campus, Aurora, CO;   [5]University of Colorado Comprehensive Cancer Center, University of Colorado Anschutz Medical Campus, Aurora, CO;   [6]Division of Hematology, University of Colorado Anschutz Medical Campus, Aurora, CO;   [7]Cancer Science Institute, National University of Singapore, Singapore;   [8]Harvard Stem Cell Institute, Harvard Medical School, Boston, MA.

Correspondence to Eric M. Pietras: eric.pietras@cuanschutz.edu;   James DeGregori: james.degregori@cuanschutz.edu.

AML-like diseases in mouse models (Bereshchenko et al., 2009; Kirstetter et al., 2008; Pabst et al., 2001b; Porse et al., 2005; Zhang et al., 1997; Zhang et al., 2004). Therefore, *CEBPA* LOF represents a common mechanism of hematopoietic dysregulation across hematologic disorders. Yet we lack insight into the mechanisms driving selection for the *CEBPA* LOF phenotype in hematologic disorders.

Analysis of steady-state hematopoiesis suggests that multipotent progenitors (MPPs) derived from hematopoietic stem cells (HSCs) are major daily contributors to blood production and are long-lived under unperturbed conditions in mice (Busch et al., 2015; Säwén et al., 2016; Sun et al., 2014). Thus, in order to understand the origin of hematologic disorders, it is important to consider both HSCs and MPPs, collectively referred to as HSPCs, as potential oncogenic reservoirs, and to appreciate how they interact with their microenvironment.

We hypothesized that because chronic exposure to IL-1 drives precocious differentiation, it may drive selection for adaptive phenotypes that counteract HSPC differentiation as achieved by *Cebpa* LOF. To test this hypothesis, we modeled the impact of chronic inflammation on competition between WT and *Cebpa*-knockout HSPCs in vivo, by treating chimeric mice with IL-1β for 20 d. *Cebpa*-knockout HSPCs are resistant to the prodifferentiative effects of IL-1β, thereby providing a fitness advantage in this setting, and leading to their preferential expansion in the bone marrow (BM). These data illustrate the potential for inflammation to alter the intrinsic transcriptional landscape of HSPCs and to drive the selective fitness of potentially oncogenic HSPCs in the BM. Finally, we explored how genes regulated by IL-1β and dependent on *Cebpa* are altered in AMLs and the impact of restored C/EBPα activity on AML fitness.

Results

HSPC-specific *Cebpa* knockout causes expansion of MPPs

To understand how *Cebpa* disruption impacts HSPC fitness in a context-dependent manner, we crossed *Cebpa*$^{f/f}$ mice (Zhang et al., 2004) with *R26R-LSL-EYFP* and *HSC-SCL-Cre-ER*^{T} transgenic mice (Göthert et al., 2005) to achieve traceable, tamoxifen-inducible, HSPC-specific knockout of *Cebpa* (herein referred to as *Cebpa*$^{Δ/Δ}$). To induce *Cebpa* excision, we treated mice with 2.5 mg tamoxifen for 3 d and analyzed mice 7 d later (Fig. 1 A). We confirmed that YFP accurately reports *Cebpa* excision by genotyping individual colonies formed on methylcellulose from YFP$^+$ HSPC-enriched Lineage$^-$Sca1$^+$cKit$^+$ (LSK) cells at 95% specificity (Fig. S1 A and not depicted). 2 d after tamoxifen treatment, the LSK population was highly and specifically labeled, followed by the appearance of YFP$^+$ cells within more differentiated populations by day 7 (Fig. S1 B).

To assess the impact of *Cebpa* knockout on hematopoietic lineage distribution in this model, we analyzed BM and peripheral blood from *Cebpa*$^{+/+}$ and *Cebpa*$^{Δ/Δ}$ mice (Fig. S1, C and D; and Fig. 1, B–F). BM cellularity was significantly reduced in *Cebpa*$^{Δ/Δ}$ mice (Fig. 1 B). *Cebpa* knockout did not significantly affect the frequency of phenotypically defined long-term HSC (LT-HSC) or short-term HSC (ST-HSC), but significantly increased the frequency of megakaryocyte/erythroid (MegE)-

biased MPP2s and granulocyte/monocyte (GM)-biased MPP3s, with a trending increase in lymphoid-biased MPP4s (Fig. 1 D). *Cebpa*$^{Δ/Δ}$ mice also had a significant buildup of MegE-lineage progenitors and GM-lineage progenitors, suggestive of a block in myeloid lineage differentiation at this level. We did not observe differences in common lymphoid progenitors (Fig. 1 D). *Cebpa*$^{Δ/Δ}$ mice had no significant changes in the frequency of mature BM cell populations (Fig. 1 E) or mature peripheral blood cells, except for a significant reduction in RBC counts (Fig. 1 F). The lack of changes in mature BM cells or in LT-HSCs or ST-HSCs differs from previous studies (Ye et al., 2013; Zhang et al., 2004). This is likely due to using an HSPC-specific Cre rather than *Mx1*-Cre, in which the effect of a differentiation block is delayed due to the slower turnover of HSCs and MPPs, and also performing analyses 7 d after deletion. This mouse model thus corroborates previous findings that C/EBPα acts during myeloid lineage specification upstream of granulocyte-monocyte progenitors (GMPs; Zhang et al., 2004) and preGMs (Pundhir et al., 2018).

HSPC-specific *Cebpa* knockout enhances MPP colony-forming potential

IL-1β promotes precocious myeloid differentiation with concomitant loss of HSC self-renewal (Pietras et al., 2016). Because *Cebpa* knockout blocks myeloid differentiation upstream of GMPs and preGMs, we hypothesized that *Cebpa*$^{Δ/Δ}$ LSK cells would retain serial replating activity when exposed to IL-1β. We sorted 100 LSK cells from *Cebpa*$^{+/+}$ or *Cebpa*$^{Δ/Δ}$ mice and performed methylcellulose CFU assays with or without IL-1β (Fig. 2 A). We assessed colony types and numbers using both morphologic scoring and flow cytometry (data not shown). While IL-1β did not affect the number of CFUs or total cell numbers from *Cebpa*$^{+/+}$ LSK cells on initial plating (Fig. 2, B and C), it did skew output toward significantly more differentiated CFU-GM colonies (both Mac1^{low}Gr1$^+$ and Mac1^{high}Gr1$^+$ by flow cytometry), with significantly fewer CFU-GEMM (mixed lineage of granulocyte, erythroid, macrophage, megakaryocyte; Lin$^-$Sca1$^-$cKit$^+$ by flow cytometry) colonies (Fig. 2 D), consistent with previous studies using purified HSCs (Pietras et al., 2016). In the absence of IL-1β, *Cebpa*$^{Δ/Δ}$ LSK cells formed significantly fewer and smaller CFUs, producing fewer mature CFU-G (Mac1^{low}Gr1$^+$ by flow cytometry) than *Cebpa*$^{+/+}$ LSK cells while retaining significantly more immature CFU-blast (Lin$^-$Sca1$^+$cKit$^+$ by flow cytometry; Fig. 2, B–D). In contrast, IL-1β significantly increased the clonogenic potential of *Cebpa*$^{Δ/Δ}$ LSK cells (Fig. 2 B), while having no significant impact on the clonogenic potential of *Cebpa*$^{+/+}$ LSK cells. Even in the presence of IL-1β, *Cebpa*$^{Δ/Δ}$ LSK cells maintained significantly more multipotent CFU-GEMM and produced fewer mature CFU-GM and CFU-G than that of *Cebpa*$^{+/+}$ (Fig. 2 D).

To functionally assess HSPC clonogenic potential, we serially replated 10^4 cells from the initial plating onto methylcellulose without IL-1β (Fig. 2 A). On the second plating, *Cebpa*$^{Δ/Δ}$ cells formed significantly more CFUs than *Cebpa*$^{+/+}$ cells, regardless of prior IL-1β exposure. *Cebpa*$^{+/+}$ cells were not maintained past the third replating, whereas *Cebpa*$^{Δ/Δ}$ cells continued to expand in number up to a fourth replating (Fig. 2 E). Since IL-1β significantly increased both the number of CFU and total cells
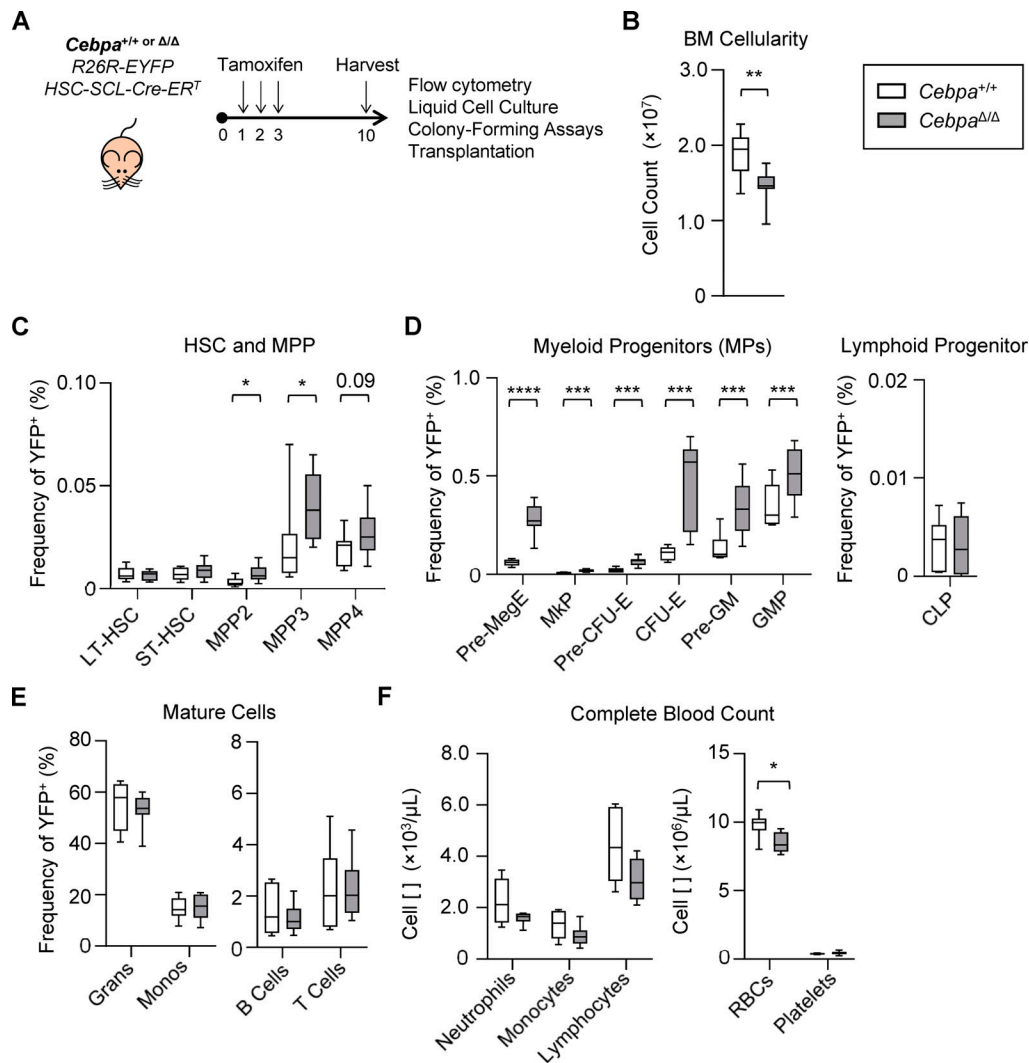
Figure 1. **HSPC-specific *Cebpa* knockout causes expansion of MPPs. (A–F)** Hematopoietic characterization of *Cebpa*^{+/+} and *Cebpa*[Δ/Δ] mice 7 d after deletion. **(A)** Schematic to achieve traceable, tamoxifen-inducible, HSPC-specific knockout of *Cebpa*. **(B)** BM cellularity from one femur and one tibia per mouse. **(C)** HSPC frequency. **(D)** Committed progenitor frequency. **(E)** Mature cell frequency. **(F)** Complete blood count. CLP, common lymphoid progenitor; LT, long-term; ST, short-term. Data are from three separate experiments with $n = 3$ per group ($n = 9$ per genotype), presented as mean ± SD, and analyzed by unpaired Mann–Whitney U test. *, $P < 0.05$; **, $P < 0.01$; ***, $P < 0.001$; ****, $P < 0.0001$.

produced from *Cebpa*[Δ/Δ] LSK cells in the initial plating (Fig. 2, B and C), we accounted for this initial expansion difference in the overall clonogenic activity of *Cebpa*[Δ/Δ] LSK cells by calculating a "cumulative CFU potential." We multiplied the total number of cells from the first plating by the CFUs formed per 10^4 cells at replating (Fig. 2 F). Using this approach, we found that IL-1β significantly increased the cumulative CFU potential of *Cebpa*[Δ/Δ] LSK cells but not *Cebpa*^{+/+} LSK cells (Fig. 2 F). Together, these data indicate that the clonogenic potential of *Cebpa*[Δ/Δ] HSPCs is potentiated by IL-1β without inducing precocious myeloid differentiation as in *Cebpa*^{+/+} cells.

Cebpa knockout confers a fitness advantage in the context of chronic IL-1β

The IL-1β–enhanced colony-forming activity we observed led us to hypothesize that IL-1β may engender a fitness advantage for *Cebpa*[Δ/Δ] LSK cells in vivo. To test this concept, we competitively

transplanted sorted LSK cells from donor *Cebpa*^{+/+} or *Cebpa*[Δ/Δ] mice with C57BL/6 (CD45.2) competitor BM into congenic Boy/J (CD45.1) recipients, allowing us to track the donor, competitor, and recipient populations by flow cytometry (Fig. 3, A and B). To isolate the effects of chronic IL-1β in the transplant setting, we used mild busulfan conditioning, which we previously showed to be less inflammatory and less disruptive to the hematopoietic system than irradiation (Henry et al., 2015). Because busulfan does not significantly deplete mature hematopoietic cells, we also treated recipients with CD4 and CD8 T cell–depleting antibodies to prevent rejection of *Cebpa*^{+/+} or *Cebpa*[Δ/Δ] donor cells expressing YFP, a potential foreign antigen. At 3 wk after transplant, we found that peripheral blood chimerism ranged between 1 and 7% and was significantly lower for *Cebpa*[Δ/Δ]-derived cells (Fig. 3 C). Thus, this system models early stages of leukemogenesis whereby rare oncogenically initiated cells must compete with more abundant normal progenitors.
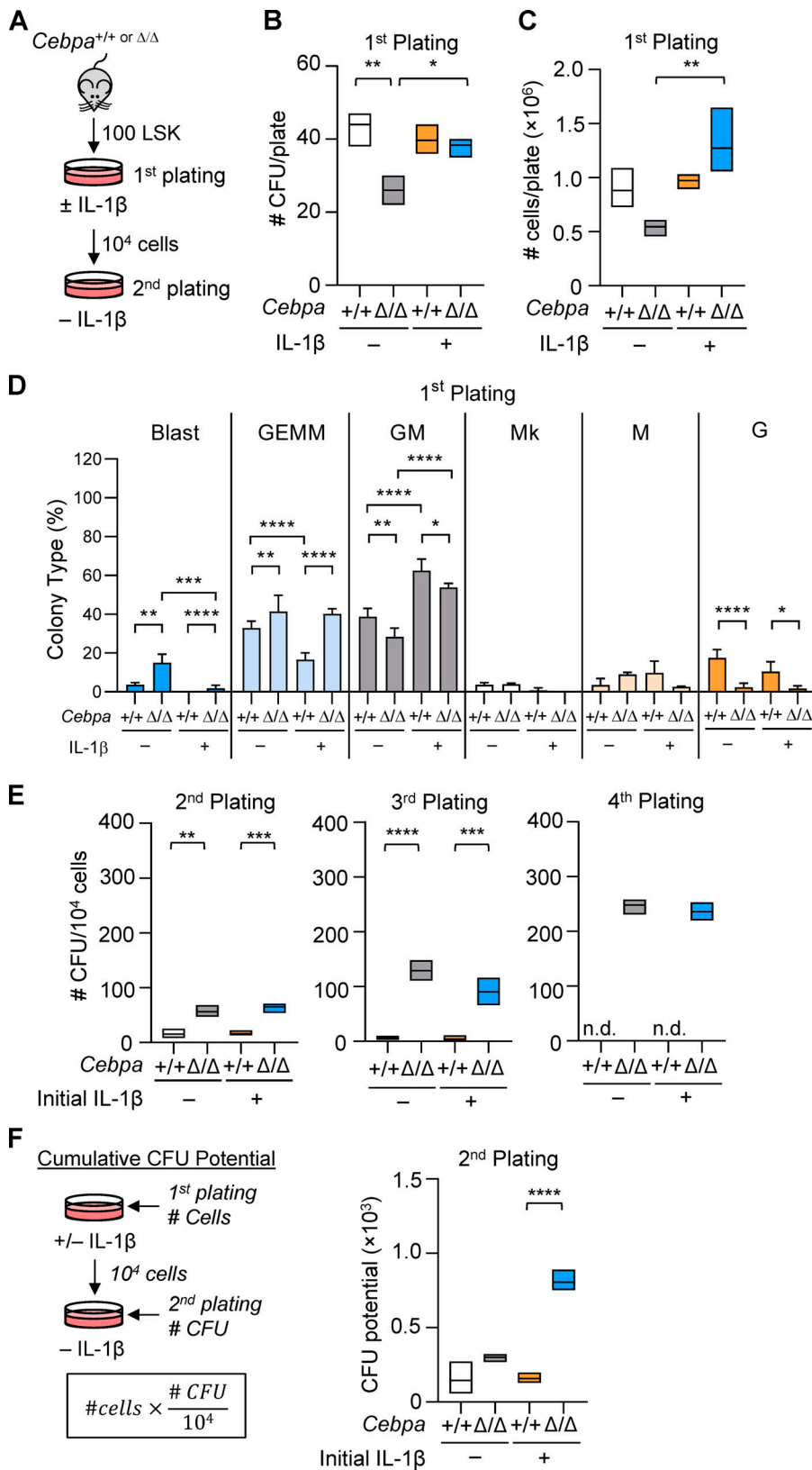
Figure 2. **HSPC-specific *Cebpa* knockout enhances MPP activity. (A)** Experimental design for LSK CFU assay. **(B–F)** LSK CFU assay data. **(B)** CFU counts per plate for initial plating. **(C)** Total cell counts per plate for initial plating. **(D)** Frequencies of CFU types for initial plating. Mk, megakaryocyte. **(E)** CFU counts per plate on replating 10^4 cells. n.d., not done because too few cells were recovered. **(F)** Calculation and data for cumulative CFU potential for second plating. Data are representative of three separate experiments with $n = 3$ per group, presented as mean ± SD, and analyzed by two-way ANOVA with Tukey's multiple comparisons test. *, $P < 0.05$; **, $P < 0.01$; ***, $P < 0.001$; ****, $P < 0.0001$. Could not perform statistics for fourth replating due to missing data points.

We subsequently treated the recipient mice ± IL-1β for 20 d (Fig. 3 A). As anticipated, chronic IL-1β treatment increased levels of inflammatory cytokines in the BM, in particular IL-1α, TNF-α, and the chemokine KC (Fig. S1 E). To confirm that our transplant conditions did not alter hematopoietic responses to IL-1β, we first assessed the hematopoietic output of WT competitor and recipient populations. As previously reported, chronic IL-1β increased production of myeloid-biased MPP3s,
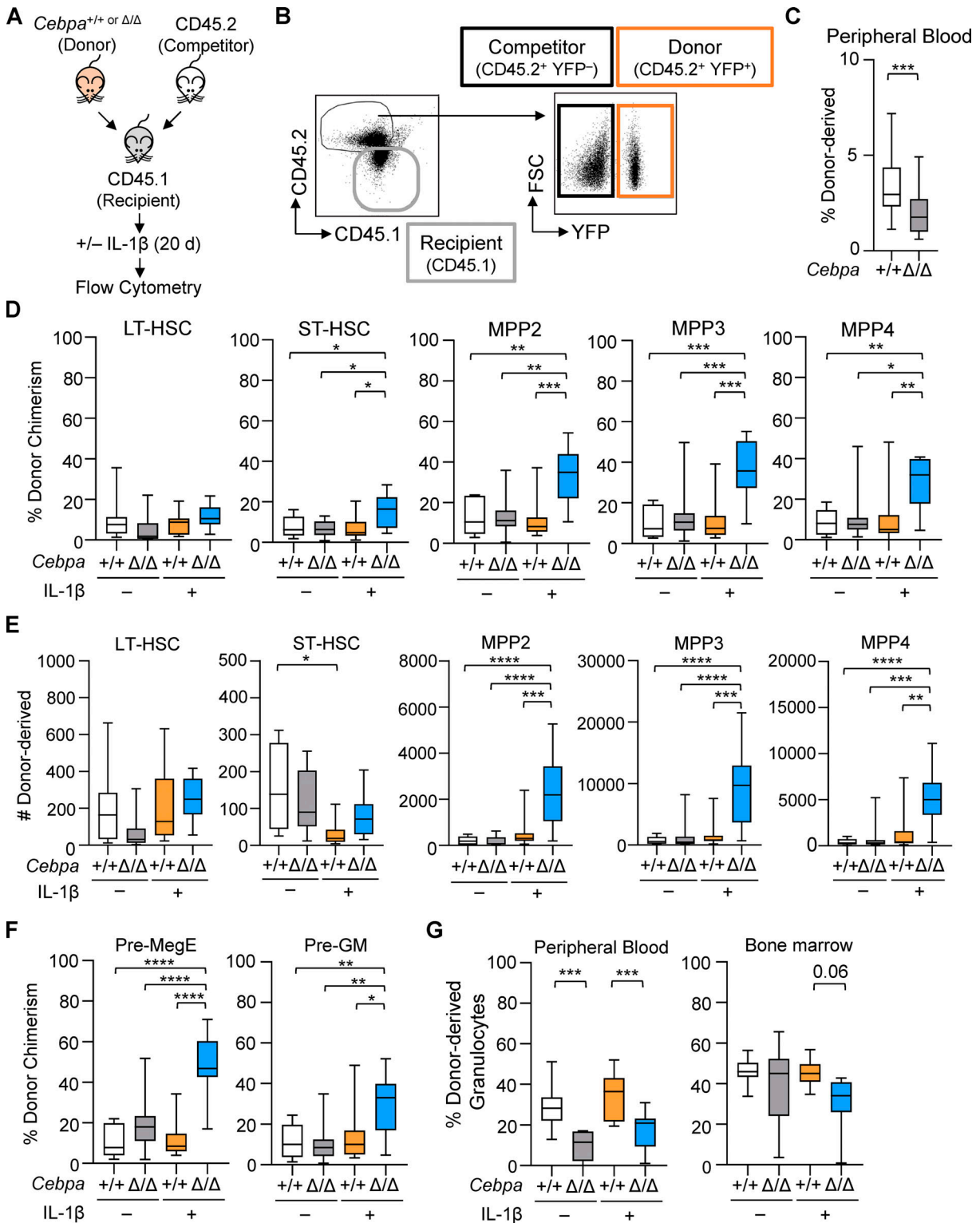
Figure 3. **Cebpa knockout confers a fitness advantage in the context of chronic IL-1β in competitive transplants. (A)** Experimental design for competitive BM transplants. **(B)** Representative flow cytometry plots to identify donor (CD45.2+YFP+), competitor (CD45.2+YFP−), and recipient (CD45.1+) populations. FSC, forward scatter. **(C)** Initial engraftment in the periphery was assessed by frequency of donor-derived (CD45.2+YFP+) leukocytes 3 wk after transplant. **(D–F)** Following 20 d of treatment with vehicle or IL-1β, BM was analyzed as follows. **(D)** Donor chimerism presented as percentage CD45.2+YFP+ of each indicated HSPC population. LT, long-term; ST, short-term. **(E)** Absolute numbers of donor-derived (CD45.2+YFP+) HSPCs in the BM from one femur and one tibia per mouse. **(F)** Donor chimerism presented as percentage CD45.2+YFP+ of each indicated myeloid progenitor population. **(G)** Granulocyte derived from donors in peripheral blood and BM. Data are representative of three separate experiments with n = 10 per group, presented as mean ± SD, and analyzed by unpaired Mann–Whitney U test (C) and two-way ANOVA with Tukey's multiple comparisons test (D–G). *, P < 0.05; **, P < 0.01; ***, P < 0.001; ****, P < 0.0001.

Higa et al.   Journal of Experimental Medicine   5 of 20

Interleukin-1–mediated selection for Cebpa loss   https://doi.org/10.1084/jem.20200560

GMPs, and granulocytes (Fig. S2, A and B; Pietras et al., 2016). We next evaluated competition dynamics within HSCs, MPPs, and myeloid progenitors by assessing donor, recipient, and competitor chimerism within each compartment (Fig. 3, D and F; and Fig. S2, C and D). Importantly, in the absence of chronic IL-1β, $Cebpa^{+/+}$ and $Cebpa^{Δ/Δ}$ donor chimerism was equivalent, suggesting that the $Cebpa^{Δ/Δ}$ LSK population does not possess a hematopoietic cell intrinsic competitive advantage (Fig. 3 D). In contrast, chronic IL-1β administration triggered selective expansion of donor-derived $Cebpa^{Δ/Δ}$ ST-HSC, MPP2, MPP3, and MPP4 compartments (Fig. 3 D). This expansion was also reflected in the absolute number of donor-derived $Cebpa^{Δ/Δ}$ MPPs, with the largest numerical expansion occurring within the MPP3 fraction (Fig. 3 E). Chronic IL-1β–dependent expansion of donor-derived $Cebpa^{Δ/Δ}$ cells likewise occurred in downstream preMegE and preGM populations (Fig. 3 F). On the other hand, at this time point we observed significant deficits in $Cebpa^{Δ/Δ}$ donor-derived granulocytes in the periphery (Fig. 3 G), consistent with a block in myeloid differentiation. Hence, by using less inflammatory methods for transplant, we did not see any evidence of cell-intrinsic competitive advantage in $Cebpa^{Δ/Δ}$ LSK cells. On the other hand, chronic inflammatory signaling via IL-1β triggered selective expansion of $Cebpa^{Δ/Δ}$ HSPCs in our model.

Withdrawal of IL-1β eliminates the fitness advantage of *Cebpa*-knockout HSPC

The effects of IL-1β on HSCs are reversible, as HSC self-renewal and balanced myeloid and lymphoid differentiation are recovered upon withdrawal of IL-1β (Pietras et al., 2016). Thus, we hypothesized that the competitive advantage of *Cebpa*-knockout HSPCs would likewise be dampened upon withdrawal of IL-1β. To test this, we performed competitive transplants and treated recipient mice with IL-1β for 20 d as described above, and then allowed the recipient mice to rest without treatment for an additional 20 d (Fig. 4 A). Consistent with our prediction, we found no difference in $Cebpa^{+/+}$ and $Cebpa^{Δ/Δ}$ chimerism within the LT-HSC, ST-HSC, MPP2, MPP3, or MPP4 compartments or within mature cell compartments after withdrawal of IL-1β (Fig. 4, B and C). These data suggest that withdrawal of IL-1β eliminates the fitness advantage of *Cebpa*-knockout HSPCs, supporting a model in which selective expansion of these cells requires ongoing exposure to inflammatory signals.

Chronic IL-1β–driven myeloid gene programs are *Cebpa* dependent

As shown above in Fig. 3, the $Cebpa^{Δ/Δ}$ MPP3 compartment exhibited the most striking expansion during chronic IL-1β exposure. Because chronic IL-1β and *Cebpa* knockout are likely to exert opposing effects on myeloid lineage output, we chose to investigate the molecular mechanism by which $Cebpa^{Δ/Δ}$ confers a fitness advantage on the GM-biased MPP3 compartment in the context of chronic IL-1β exposure. Thus, we isolated both donor- and competitor-derived MPP3s from recipient mice and performed RNA sequencing (RNA-seq; Fig. 5 A). After validating *Cebpa* knockout by assessing its transcript levels in donor-derived MPP3s (Fig. S3 A), we determined the gene expression

consequences of *Cebpa* deficiency in MPP3s (Fig. S3 B). There were 494 differentially expressed genes (adjusted P < 0.05) between $Cebpa^{Δ/Δ}$ and $Cebpa^{+/+}$ MPP3s isolated from vehicle-treated mice (Fig. S3 B; gene list in Table S1). Chronic IL-1β had little effect on the relative expression of these genes between $Cebpa^{Δ/Δ}$ and $Cebpa^{+/+}$ MPP3s, suggesting that loss of *Cebpa* is epistatic to chronic IL-1β (Fig. S3 B). We then focused on chronic IL-1β–driven gene expression changes by comparing gene expression in $Cebpa^{+/+}$ MPP3s isolated from recipient mice treated with or without chronic IL-1β. There were 555 differentially expressed genes (adjusted P < 0.05). Interestingly, chronic IL-1β failed to induce most gene expression changes in *Cebpa*-knockout MPP3s, suggesting that *Cebpa* is required for the majority of chronic IL-1β–induced gene programs in MPP3s (Fig. 5 B). Only a small subset of chronic IL-1β–induced gene expression changes were independent of *Cebpa* (Fig. 5 B). *Il1r1* expression was unchanged in $Cebpa^{Δ/Δ}$ MPP3s, ruling out the lack of IL-1 signaling as an explanation for the attenuated transcriptional signature (Fig. S3 A).

To gain insight into the biological impact of these gene expression changes, we performed overrepresentation analysis (ORA) on genes grouped based on whether they were significantly up- or down-regulated by chronic IL-1β and whether this change was *Cebpa* dependent or independent (Fig. 5 C). From the chronic IL-1β up-regulated genes that are dependent on *Cebpa*, 61 pathways were overrepresented with adjusted P < 0.05 (Fig. 5 C), with many related to myeloid lineage or immunity. In accordance with ORA, pairwise gene set enrichment analyses (GSEA) revealed that *Cebpa* knockout prevented activation of myeloid gene programs despite chronic IL-1β exposure (Fig. 6, A–C; and Fig. S3 C). These data are consistent with the failure of donor-derived $Cebpa^{Δ/Δ}$ to overproduce granulocytes in response to chronic IL-1β (Fig. 3 G).

Additional pathways that chronic IL-1β up-regulates in a *Cebpa*-dependent manner included those related to metabolism, protein synthesis, and redox homeostasis (Fig. 5 C; Fig. 6, A–C; and Fig. S3 C). Multiple studies have shown that tight regulation of these pathways is required for HSC function (García-Prat et al., 2017; Ito and Suda, 2014; Signer et al., 2014). For instance, mTORC1 signaling, which is an important regulator of cell growth by regulating protein synthesis and cellular metabolism, has been shown to be important for myeloid cell differentiation (Peng et al., 2018; Zhang et al., 2019), and its hyperactivation can lead to HSC exhaustion (Gan and DePinho, 2009). HSPC differentiation is likewise associated with increased metabolic and biosynthetic demands, so it seems appropriate that chronic IL-1β priming of MPP3s for myeloid differentiation is associated with up-regulation of the cellular processes required for differentiation. These data underscore the role of *Cebpa* as a master regulator coordinating not only myeloid gene programs, but also gene programs for cellular processes required to support differentiation.

Chronic IL-1β–induced *Cebpa*-knockout MPP3 expansion is cell cycle independent

IL-1β can stimulate HSPC proliferation (Pietras et al., 2016; Ueda et al., 2009; Weisser et al., 2016). Conversely, C/EBPα inhibits
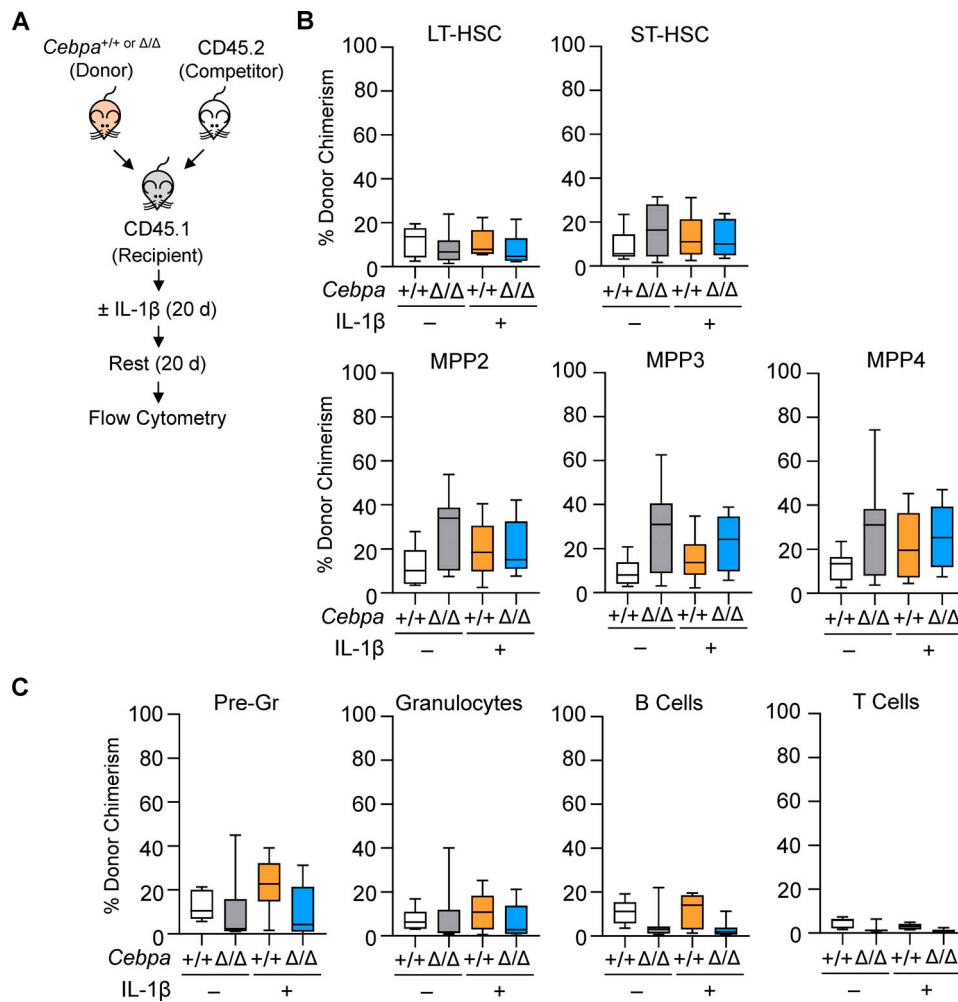
Figure 4. **Withdrawal of IL-1β eliminates the fitness advantage of *Cebpa*-knockout HSPCs. (A)** Experimental design for competitive BM transplant. **(B and C)** After treatment with vehicle or IL-1β for 20 d and subsequent withdrawal of treatment for 20 d, BM was analyzed as follows. **(B)** Donor chimerism presented as percentage CD45.2+YFP+ of each indicated HSPC population. LT, long-term; ST, short-term. **(C)** Donor chimerism presented as percentage CD45.2+YFP+ of each indicated mature cell population. Data are from two separate experiments with *n* = 3–5 per group, presented as mean ± SD, and analyzed by two-way ANOVA with Tukey's multiple comparisons test. No comparisons were significant.

cell cycle entry through direct interaction with cyclin-dependent kinases and E2F (Johnson, 2005), and *Cebpa*-knockout HSCs exhibit loss of quiescence (Hasemann et al., 2014; Ye et al., 2013). Thus, we reasoned that chronic IL-1β may directly activate increased *Cebpa*^Δ/Δ MPP3 proliferation, resulting in their selective expansion. Unexpectedly, *Cebpa* knockout actually prevented chronic IL-1β–driven up-regulation of mTORC1 and cell cycle genes associated with cell proliferation (Fig. 6, A–C). Consistent with our gene expression data, cell cycle analysis of donor-derived *Cebpa*^+/+ and *Cebpa*^Δ/Δ MPP3s isolated from recipient mice treated with or without chronic IL-1β revealed a modest but significant increase in the frequency of *Cebpa*^+/+ MPP3s in S/G2/M phase following treatment with chronic IL-1β, whereas the cell cycle status of *Cebpa*^Δ/Δ MPP3s was un-changed relative to controls (Fig. 6, D–F). Together, these data suggest that the competitive advantage of *Cebpa*^Δ/Δ MPP3s in the presence of IL-1β is not explained by changes in cell cycle activity.

Chronic IL-1β triggers a self-renewal gene program in *Cebpa*-knockout MPP3s

To further assess the molecular basis for selective expansion of *Cebpa*^Δ/Δ MPP3s in vivo, we analyzed genes down-regulated by IL-1β in *Cebpa*^+/+ but not *Cebpa*^Δ/Δ MPP3s. ORA revealed that pathways with this expression pattern included those related to stemness (Fig. 5 C), suggesting that chronic IL-1β represses stem cell gene programs in MPP3 via a C/EBPα–dependent mechanism. GSEA supported these findings, showing enrichment for stem cell gene signatures in *Cebpa*^Δ/Δ MPP3s from chronic IL-1β–treated recipient mice (Fig. 7, A–C; and Fig. S3 C). To validate these findings, we isolated donor-derived *Cebpa*^+/+ and *Cebpa*^Δ/Δ MPP3s from recipient mice treated with or without chronic IL-1β and performed quanti-tative RT-PCR analysis using a custom Fluidigm gene expression array (Fig. 7 D). We found that expression of genes essential for HSC self-renewal, such as *Bmi1*, *Foxo3*, *Mpl*, and *Mycn* (Iwama et al., 2004; Laurenti et al., 2008; Miyamoto et al., 2007; Nitta et al., 2020; Yoshihara et al., 2007), were elevated in *Cebpa*^Δ/Δ MPP3s as com-pared with *Cebpa*^+/+ MPP3s from chronically IL-1β–exposed mice
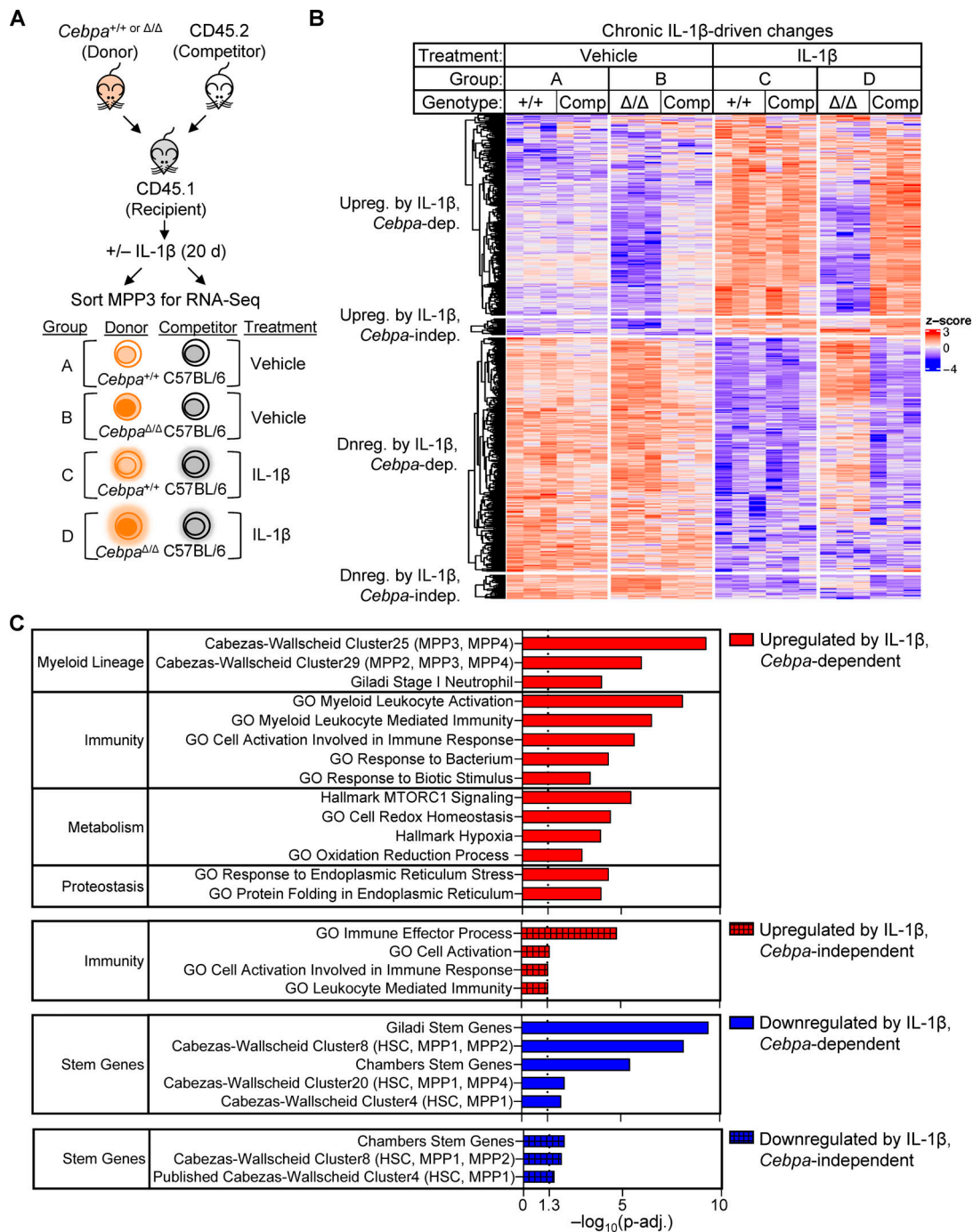
Figure 5. **Cebpa mediates many of the chronic IL-1β gene expression changes. (A)** Experimental design for RNA-seq (n = 3 of 3–4 mice pooled to obtain 2,000 donor [CD45.2+YFP+] or competitor [CD45.2+YFP−] MPP3s). **(B)** Heatmap of all genes significantly changed (adjusted P < 0.05) by chronic IL-1β, grouped based on pattern of expression: up-regulated (upreg.) with IL-1β, *Cebpa*-dependent; upreg. with IL-1β, *Cebpa*-independent; down-regulated (dnreg.) with IL-1β, *Cebpa*-dependent; dnreg. with IL-1β, *Cebpa*-independent (genes for heatmap are listed in Table S1). **(C)** Table showing select significant pathways (adjusted P < 0.05) from ORA.

(Fig. 7 E). Thus, the fitness advantage in the context of chronic IL-1β may be attributed to a coordinate increase in self-renewal–associated genes in *Cebpa*Δ/Δ MPP3s.

IL-1β triggers aberrant expansion potential of *Cebpa*-knockout MPP3s

To assess the direct impact of IL-1β on *Cebpa*+/+ or *Cebpa*Δ/Δ MPP3 expansion, we sorted MPP3s from primary *Cebpa*+/+ or *Cebpa*Δ/Δ

mice for liquid culture with or without IL-1β and assessed MPP3 maintenance and differentiation by flow cytometry (Figs. 7 F and S4 A). Similar to studies performed with purified HSCs (Pietras et al., 2016), IL-1β induced precocious differentiation of *Cebpa*+/+ MPP3s and early accumulation of Mac1+Gr1+ cells (Fig. 7 G). This was associated with a concomitant early depletion of MPP3s, resulting in significantly reduced differentiation potential at day 8 (Fig. 7, G and H). Despite IL-1β treatment, *Cebpa*Δ/Δ MPP3s
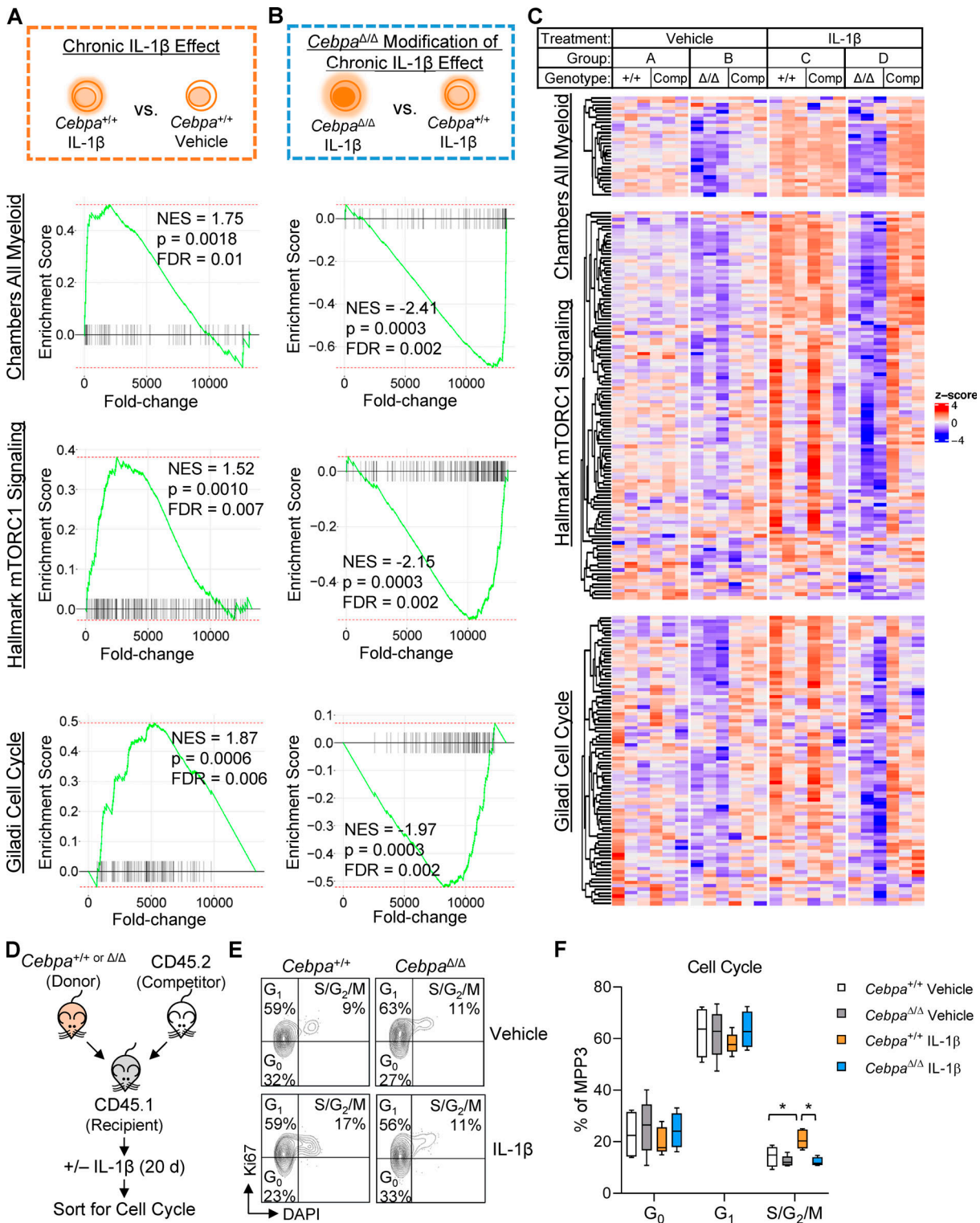
Figure 6. ***Cebpa* knockout counteracts chronic IL-1β–driven transcriptional programs. (A–C)** GSEA using "Chambers all myeloid," "hallmark mTORC1 signaling," and "Giladi cell cycle" gene sets. **(A)** Schematic and enrichment plots for pairwise comparison between *Cebpa*^+/+^ MPP3 isolated from chronic IL-1β–treated versus vehicle-treated mice ("chronic IL-1β effect"). **(B)** Schematic and enrichment plots for pairwise comparison between *Cebpa*^Δ/Δ^ and *Cebpa*^+/+^ MPP3s isolated from chronic IL-1β–treated mice ("*Cebpa*^Δ/Δ^ modification of chronic IL-1β effect"). **(C)** Heatmaps for leading edge genes from B (genes for heatmap are listed in Table S1). **(D)** Experimental design for cell cycle analysis (*n* = 5 per group). **(E)** Representative flow cytometry plots for Ki67/DAPI cell cycle analysis. **(F)** Graph of frequency of MPP3 in G0, G1, S/G2/M. FDR, false discovery rate; NES, normalized enrichment score. In D–F, cell cycle data are from one experiment with *n* = 5 mice per group, presented as mean ± SD, and analyzed by two-way ANOVA with Tukey's multiple comparisons test. *, P < 0.05; **, P < 0.01.
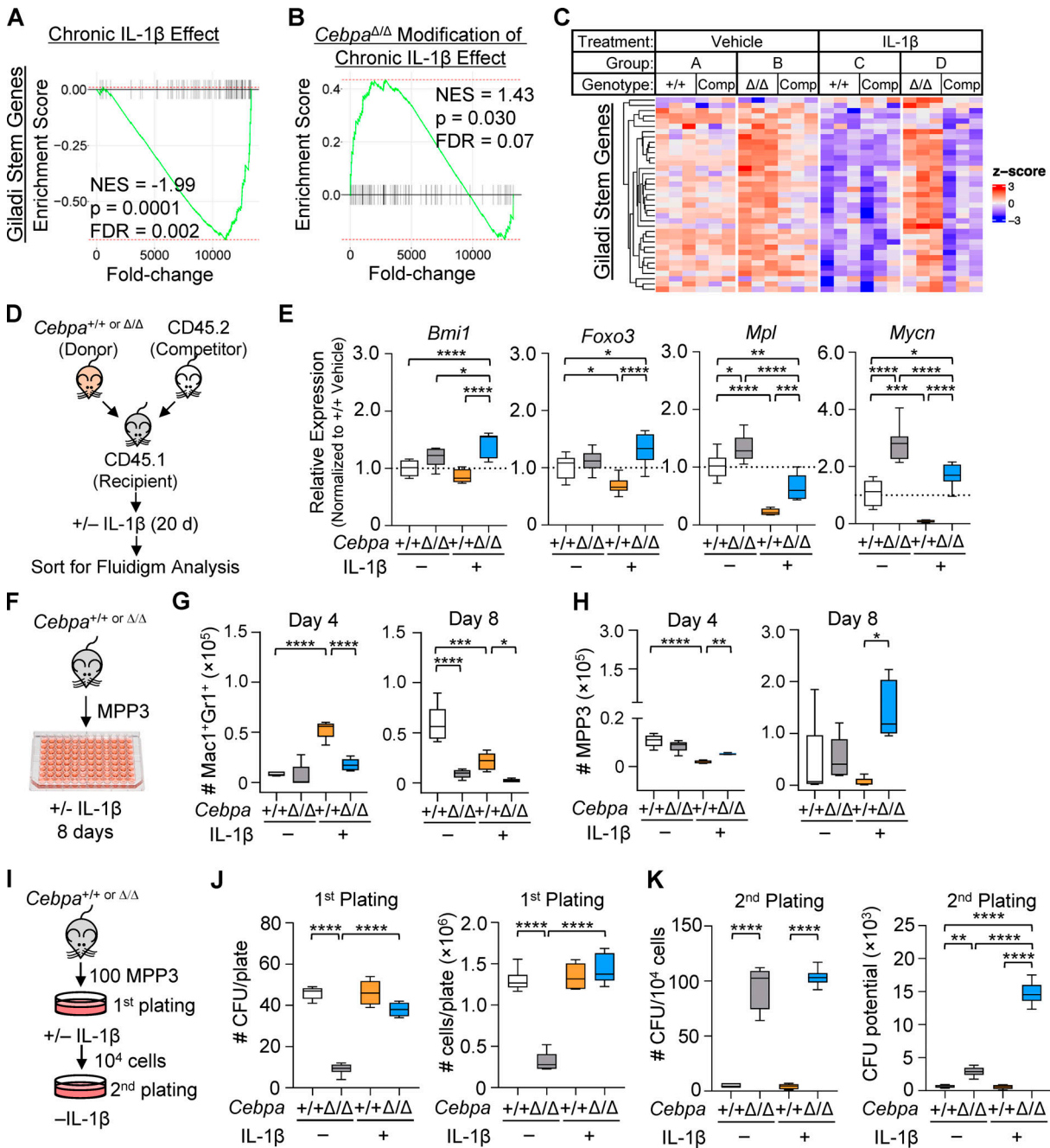
Figure 7. **Chronic IL-1β triggers aberrant expansion potential of *Cebpa*-knockout MPP3. (A–C)** GSEA using "Giladi stem genes" gene set. **(A)** Schematic and enrichment plot for pairwise comparison between *Cebpa*⁺/⁺ MPP3 isolated from chronic IL-1β–treated versus vehicle-treated mice ("chronic IL-1β effect"). **(B)** Schematic and enrichment plot for pairwise comparisons between *Cebpa*^Δ/Δ versus *Cebpa*⁺/⁺ MPP3 isolated from chronic IL-1β–treated mice ("*Cebpa*^Δ/Δ modification of chronic IL-1β effect"). **(C)** Heatmap for leading edge genes from B (genes for heatmap are provided in Table S1). **(D)** Experimental design for Fluidigm Biomark gene expression analysis (one experiment independent from RNA-Seq, eight replicates from $n = 5$ pooled mice per group). **(E)** Relative expression of self-renewal genes (*Bmi1*, *Foxo3*, *Mpl*, and *Mycn*) calculated by first normalizing to *Gusb* within each group, then normalizing to *Cebpa*⁺/⁺ vehicle group. **(F–H)** Liquid culture data representative of three separate experiments with $n = 3$–5 per group. **(F)** Experimental design for MPP3 liquid culture. **(G)** Time course of Mac1⁺Gr1⁺ absolute numbers. **(H)** Time course of MPP3 absolute numbers. **(I–K)** CFU assay representative of two experiments with $n = 3$ or 6 per group. **(I)** Experimental design for MPP3 CFU. **(J)** CFU counts per plate and total cell counts per plate from initial plating. **(K)** CFU counts per plate upon replating 10^4 cells and calculated cumulative CFU potential from second plating. FDR, false discovery rate; NES, normalized enrichment score. Data are presented as mean ± SD and analyzed by two-way ANOVA with Tukey's multiple comparisons test. *, $P < 0.05$; **, $P < 0.01$; ***, $P < 0.001$; ****, $P < 0.0001$, except in G and H, in which symbols for different comparisons are indicated.

formed very few differentiated Mac1⁺Gr1⁺ cells over the 8-d culture (Fig. 7 G). Consistent with our in vivo data, there was no difference in the number of phenotypic *Cebpa^(+/+)* or *Cebpa^(Δ/Δ)* MPP3 cells after 8 d of culture without IL-1β. However, IL-1β induced selective expansion of *Cebpa^(Δ/Δ)* MPP3s in culture (Fig. 7 H). *Cebpa^(Δ/Δ)* MPP3s cultured with IL-1β also expressed elevated levels of HSC self-renewal genes identified in our in vivo studies, including *Bmi1*, *Foxo3*, *Mpl*, and *Mycn* (Fig. S4 B).

We also analyzed serial CFU activity of *Cebpa^(+/+)* or *Cebpa^(Δ/Δ)* MPP3s with or without IL-1β (Fig. 7 I). As seen with LSK cells, IL-1β did not affect the total number of CFUs or cells formed by *Cebpa^(+/+)* MPP3s on the initial round of plating. While *Cebpa^(Δ/Δ)* MPP3s formed fewer CFUs and had fewer total cells in the absence of IL-1β, their clonogenic activity increased significantly when cultured with IL-1β (Fig. 7 J). Upon replating, *Cebpa^(+/+)* cells formed very few CFUs, but *Cebpa^(Δ/Δ)* cells formed significantly more CFUs regardless of whether previously plated with or without IL-1β (Fig. 7 K), and *Cebpa^(Δ/Δ)* MPP3s retained clonogenic potential up to the third and fourth replatings (Fig. S4 C). Again, we calculated the cumulative CFU potential at replating and found that IL-1β significantly increased the cumulative CFU potential of *Cebpa^(Δ/Δ)* MPP3s (Fig. 7 K). This demonstration of IL-1β–specific *Cebpa^(Δ/Δ)* MPP3 expansion in cell culture recapitulates our in vivo data and further isolates the fitness advantage as reliant specifically on IL-1β. In addition, these data suggest that *Cebpa^(Δ/Δ)* MPP3s expand following IL-1β exposure via triggering aberrant self-renewal activity, which is consistent with up-regulation of key stem genes in vivo.

Cebpa knockout exacerbates chronic IL-1β gene programs in competitor MPP3s

Somatic cell fitness describes how cell-intrinsic properties (*Cebpa* knockout) interact with microenvironmental factors (IL-1β) and other cells within its niche. Cell competition dynamics are appreciated to be an important factor in tumorigenesis (Bowling et al., 2019). We hypothesized that WT competitor MPP3 would exhibit differential gene expression in competition against a more fit population (versus *Cebpa^(Δ/Δ)* MPP3 in chronic IL-1β) versus in neutral competition (versus *Cebpa^(+/+)* MPP3 in chronic IL-1β), even though they are identical by genotype and treatment. We performed GSEA pairwise comparisons between WT competitor MPP3s transplanted with *Cebpa^(+/+)* or *Cebpa^(Δ/Δ)* in the context of chronic IL-1β (Fig. S3 D). Interestingly, WT MPP3s that were competed against *Cebpa^(Δ/Δ)* MPP3s had enrichment for myeloid gene programs above that of WT MPP3s that were competed against *Cebpa^(+/+)* MPP3s in the context of chronic IL-1β. Further, WT MPP3s that were competed against *Cebpa^(Δ/Δ)* MPP3s exhibited reduced expression of stem gene programs as compared with WT MPP3s competed against *Cebpa^(+/+)* MPP3s in the context of chronic IL-1β (Fig. S3 D). When the same comparison was made between competitors isolated from vehicle-treated mice, we observed no enrichment for myeloid genes and much less enrichment for stem genes in the WT MPP3s competed against *Cebpa^(Δ/Δ)* MPP3s (Fig. S3 E). This suggests that WT competitors differ in gene expression only when in the presence of a fitness differential. These data provide evidence at the molecular level that

competition in the presence of *Cebpa^(Δ/Δ)* MPP3s exacerbated chronic IL-1β activation of myeloid gene programs and repression of stem gene programs.

Cebpa-dependent IL-1 target genes are enriched for C/EBPα and PU.1 binding sites

C/EBPα act both independently and cooperatively with PU.1 to regulate GM-lineage gene programs in HSPCs and can regulate PU.1 levels (Pundhir et al., 2018). To better understand how *Cebpa*-dependent genes are regulated in our system, we mined publicly available C/EBPα and PU.1 chromatin immunoprecipitation sequencing (ChIP-seq) data from LSK, preGM, GMP, and granulocytes from *Cebpa^(+/+)* and *Cebpa^(Δ/Δ)* mice (Pundhir et al., 2018). We first determined the enrichment between the genes in each binding category and genes that are up- or down-regulated by chronic IL-1β in a *Cebpa*-dependent manner. We found that genes up-regulated by chronic IL-1β in a *Cebpa*-dependent manner, which were largely related to myeloid lineage or immunity (Fig. 5, B and C), were highly enriched for C/EBPα-, PU.1-, and dual-bound regions in LSK, preGM, GMP, and granulocytes (Fig. 8 A). Genes down-regulated by chronic IL-1β in a C/EBPα-dependent manner, enriched in stem gene pathways (Fig. 5, B and C), were significantly enriched for C/EBPα-, PU.1-, and dual bound regions in preGM and GMP, but not granulocytes (Fig. 8 A). On the other hand, these genes were significantly enriched for PU.1 in LSK, preGM, and GMP (Fig. 8 A), consistent with reduced *Spi1* expression in IL-1–exposed *Cebpa^(Δ/Δ)* MPP3s (Fig. S3 A). These data support a model in which loss of *Cebpa* may (at least in part) indirectly prevent differentiation-associated down-regulation of stem cell genes via failure to induce appropriate levels of PU.1 expression. When we further analyzed genes regulated by IL-1β in a C/EBPα-dependent manner based on functional categories, we observed significant enrichment for C/EBPα binding to promoters of stem cell, myeloid, and mTORC1 pathway genes across the differentiation spectrum (except for stem cell genes in granulocytes), while binding to cell cycle promoters was not evident, suggesting indirect regulation of these genes (Fig. 8 B). Taken together, these data suggest that the *Cebpa*-dependent IL-1β–regulated genes are broadly regulated by direct binding by C/EBPα, PU.1, or both.

The *Cebpa*-dependent IL-1β–regulated gene signature is enriched in previously irradiated (IR^P) HSPCs

Our laboratory had previously shown that months after γ-irradiation exposure, HSPCs exhibit precocious differentiation and impaired self-renewal, and that prior irradiation selects for loss of *Cebpa* within the HSPC compartment (Fleenor et al., 2015b). Because the IR^P HSPC phenotype is similar to HSPCs exposed to chronic IL-1β, we hypothesized that the *Cebpa*-dependent IL-1β–regulated gene signature would be enriched in IR^P HSPCs. We performed ORA on RNA-seq performed on cultured LSK cells isolated from IR^P or unirradiated control mice (Fleenor et al., 2015b). We found that *Cebpa*-dependent IL-1β–down-regulated genes (e.g., stemness genes) were overrepresented in genes significantly down-regulated in IR^P LSK cells ($P = 2.79 \times 10^{-6}$), and *Cebpa*-dependent IL-1β–up-regulated genes
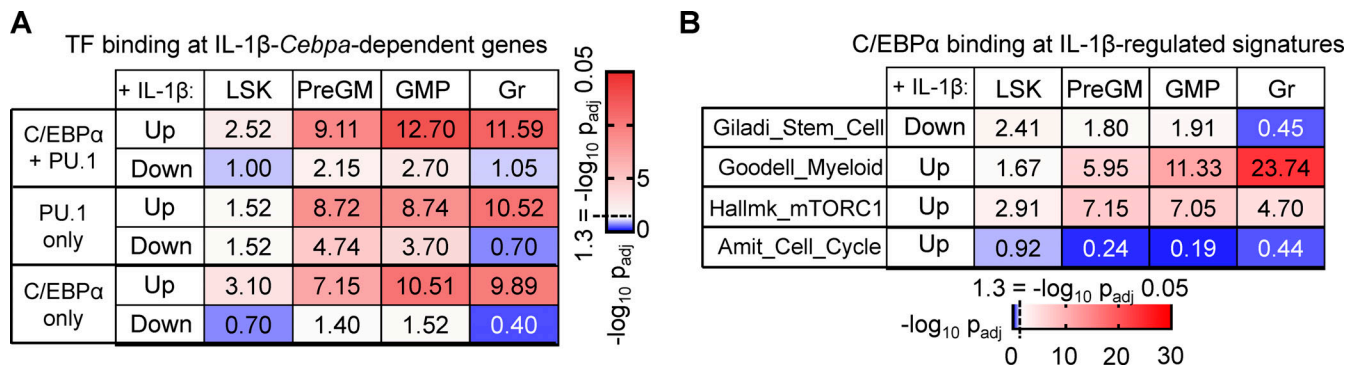
A

TF binding at IL-1β-*Cebpa*-dependent genes

+ IL-1β:		LSK	PreGM	GMP	Gr
C/EBPα + PU.1	Up	2.52	9.11	12.70	11.59
	Down	1.00	2.15	2.70	1.05
PU.1 only	Up	1.52	8.72	8.74	10.52
	Down	1.52	4.74	3.70	0.70
C/EBPα only	Up	3.10	7.15	10.51	9.89
	Down	0.70	1.40	1.52	0.40

$1.3 = -\log_{10} p_{adj}\ 0.05$

$-\log_{10} p_{adj}$

B

C/EBPα binding at IL-1β-regulated signatures

+ IL-1β:		LSK	PreGM	GMP	Gr
Giladi_Stem_Cell	Down	2.41	1.80	1.91	0.45
Goodell_Myeloid	Up	1.67	5.95	11.33	23.74
Hallmk_mTORC1	Up	2.91	7.15	7.05	4.70
Amit_Cell_Cycle	Up	0.92	0.24	0.19	0.44

$1.3 = -\log_{10} p_{adj}\ 0.05$

$-\log_{10} p_{adj}$

0 10 20 30

Figure 8. **IL-1β-*Cebpa*–dependent genes are highly enriched for C/EBPα and PU.1 binding sites. (A)** Table summarizing C/EBPα-, PU.1-, and dual-bound regions at genes that are up- or down-regulated by chronic IL-1β in a *Cebpa*-dependent manner in LSK, preGM, GMP, and granulocytes. **(B)** Table summarizing C/EBPα binding for IL-1β-*Cebpa*–dependent gene within indicated gene sets in LSK, preGM, GMP, and granulocytes.

(e.g., myeloid differentiation and cell cycle genes) were over-represented in genes significantly up-regulated in IR^P LSK cells (P = 5.0 × 10^{-4}). These data suggest that the IR^P phenotype in HSPCs may in part be driven by a *Cebpa*-dependent IL-1β–regulated gene program.

The *Cebpa*-dependent IL-1β gene signature is associated with AML subtype

CEBPA LOF occurs frequently in hematologic malignancies. As our data indicate that *Cebpa* is crucial for IL-1β–mediated HSPC differentiation, we hypothesized that the *Cebpa*-dependent IL-1β–regulated gene signature we identified would correlate with the differentiation status of AML. Historically, AML has been classified using the French–American–British (FAB) classification scheme, where M0 represents the most undifferentiated AML and M5 represents the most differentiated, monocytic-type AML (Bennett et al., 1985). Importantly, *CEBPA* mutations are commonly associated with primitive M1 and M2 FAB subtypes (Green et al., 2010; Dufour et al., 2012). Thus, we mined publicly available gene expression databases of AML samples from The Cancer Genome Atlas (TCGA; Cerami et al., 2012) and Beat AML (Tyner et al., 2018) and assigned each AML a *Cebpa*-dependent IL-1β–regulated gene score, where a higher score is determined by greater expression of *Cebpa*-dependent IL-1β–up-regulated genes (e.g., myeloid differentiation and cell cycle genes) and lesser expression of *Cebpa*-dependent IL-1β–down-regulated genes (e.g., stemness genes; Fig. 9 A). Interestingly, and consistent with the association between *Cebpa* mutations and primitive FAB subtypes, we found that the primitive M0–M2 subtypes were significantly associated with a lower *Cebpa*-dependent IL-1β–regulated gene score, whereas the M5 differentiated subtype corresponded to a higher score (Fig. 9 B). Similar results were seen for AML samples from Beat AML (data not shown).

Previous studies have shown that AML at relapse is enriched for leukemia stem cells, as demonstrated via limiting dilution transplantation experiments (Ho et al., 2016). Analyses of the Beat AML datasets reveals that the *Cebpa*-dependent IL-1β–regulated gene score is higher in AMLs at diagnosis than at relapse, consistent with enrichment for stem cell activity (Fig. 9 C). The score was similarly lower for AMLs secondary to

MDS or MPN (Fig. 9 C). While speculative at present, the inflammation associated with therapy or prior MDS/MPN may select for *Cebpa* loss, contributing to the more primitive phenotypes of relapse and secondary AMLs.

Ectopic CEBPA expression induces differentiation and impairs fitness of AML cells

Because a low *Cebpa*-dependent IL-1β gene score correlated with primitive AML, we hypothesized that ectopic expression of *CEBPA* in AML cells would induce differentiation and impair fitness. Overexpression of CEBPA has been shown to induce neutrophilic differentiation in U937 cells (Radomska et al., 1998) and in a mouse model of acute promyelocytic leukemia (Truong et al., 2003) and to override epigenetic reprogramming mediated by RUNX1 fusions in AMLs (Loke et al., 2018). To investigate *CEBPA* LOF in this context, we used a primary AML (AML0626) characterized as M0/M1/M2; AML cell lines MOLM-13 and EOL-1, which harbor *CEBPA* mutations (in-frame insertion and deletion, respectively) according to the Cancer Cell Line Encyclopedia (Ghandi et al., 2019); chronic myelogenous leukemia line K562 (no detectable expression of CEBPA; Radomska et al., 1998); and MOLM-14, which is from the same patient as MOLM-13 and exhibits a more differentiated phenotype (Matsuo et al., 1997). We set up competitive cell cultures using cells transduced with the empty vector or a *CEBPA*-expressing vector, both expressing GFP, versus nontransduced cells to obtain a culture containing ~25% GFP⁺ cells and cultured with and without IL-1β (Fig. 10, A and B; and Fig. S4 D). Analyses of transduced cells via Western blot demonstrated that ectopic expression roughly quadrupled C/EBPα levels in AML0626 (Fig. 10 C). We assessed the percentage of GFP⁺ cells and cell numbers at days 3–12. Across the multiple AML cell lines and primary cultures, we found that ectopic expression of *CEBPA* reduced the fraction of GFP⁺ cells and absolute number of GFP⁺ cells maintained in culture, indicative of a competitive disadvantage (Fig. 10, A and B; and Fig. S4 D). This was regardless of whether cells were cultured with or without IL-1β, suggesting that C/EBPα is epistatic to IL-1β (consistent with our gene expression data; Figs. S3 B and 5 B). Ectopic expression of *CEBPA* increased the frequency of
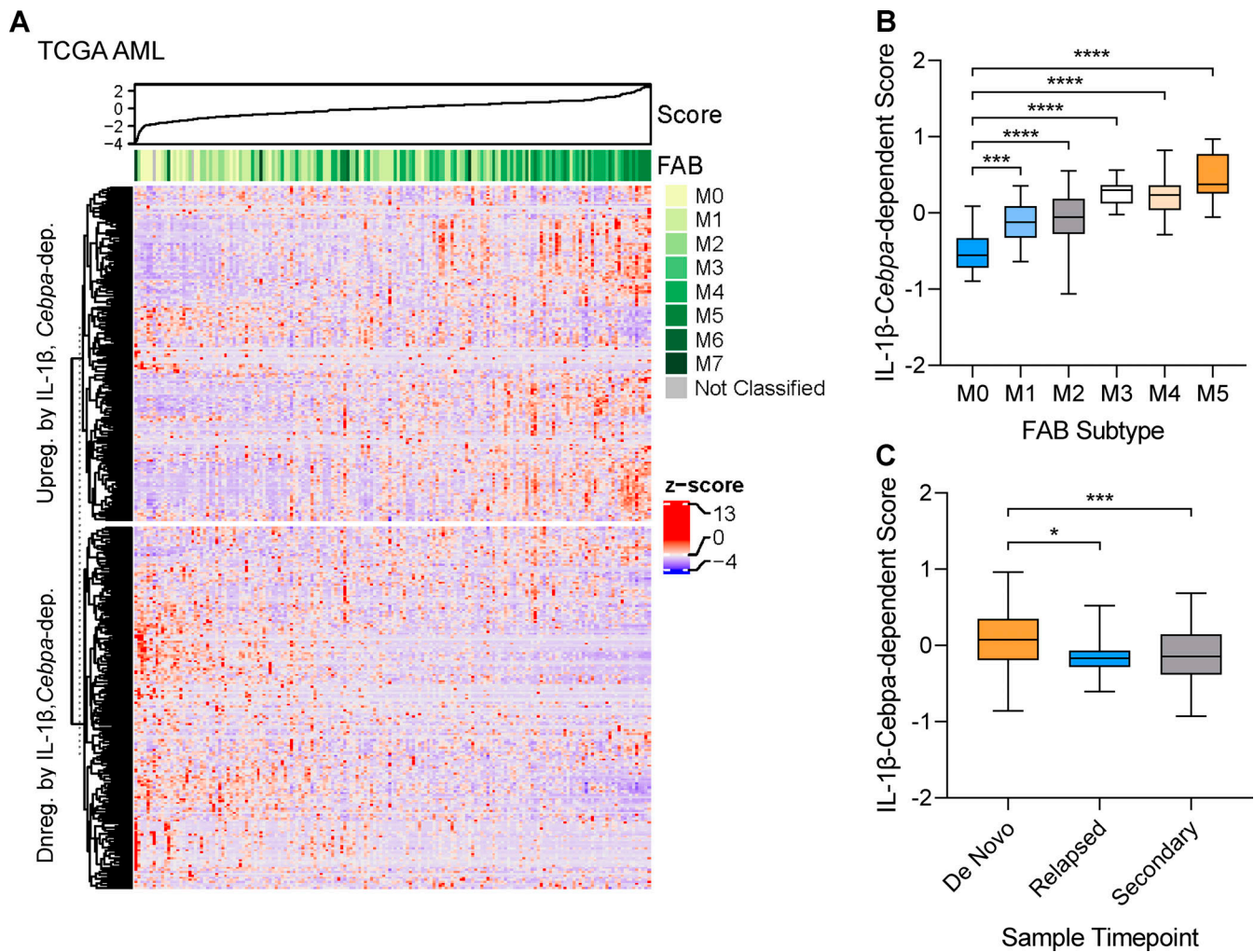
Figure 9. The IL-1β-*Cebpa*–dependent signature is associated with AML subtype. (A) Heatmap of IL-1β-*Cebpa*–dependent gene score for AML samples from TCGA. **(B)** Graph of IL-1β-*Cebpa*–dependent gene score for AML samples from TCGA by FAB subtype. **(C)** Graph of IL-1β-*Cebpa*–dependent gene score for de novo, relapse, or secondary to MDS or MPN AML samples from Beat AML. Data are presented as mean ± SD and analyzed by one-way ANOVA with Tukey's multiple comparisons test. *, P < 0.05; ***, P < 0.001; ****, P < 0.0001.

AML0626 cells expressing myeloid differentiation markers CD11b, CD14, CD15, CD16, and CD64 and reduced the frequency of cells expressing primitive cell surface markers CD34 and CD117 (Fig. 10, D and E). Notably, IL1β treatment boosted the ability of ectopic C/EBPα to increase expression of some myeloid markers such as CD16 (Fig. 10 D). Finally, GFP⁺ cells were sorted for gene expression analysis, and ectopic expression of *CEBPA* did indeed cause up-regulation of myeloid genes and down-regulation of self-renewal genes (Figs. 10 F and S4 E). Thus, the maintenance of low C/EBPα activity appears important for AML cell fitness, by reducing differentiation and increasing self-renewal.

Discussion

Using a mouse model with HSPC-specific *Cebpa* deletion and less-inflammatory competitive transplant methods, we show that *Cebpa*-knockout HSPCs do not have a hematopoietic cell intrinsic competitive advantage relative to WT HSPCs.

Strikingly, chronic IL-1β exposure triggered a fitness advantage for *Cebpa*-knockout MPPs. While chronic IL-1β remodels the HSPC compartment by expanding myeloid-biased MPPs to increase myeloid output, C/EBPα blocks myeloid differentiation. Together, these phenotypes cooperate and ultimately result in chronic IL-1β–dependent expansion of *Cebpa*^Δ/Δ cells (Fig. 10 G). While prior studies had shown an inherent competitive advantage of *Cebpa*^Δ/Δ HSCs, these investigations used polyinosinic:polycytidylic acid to induce Cre recombination and lethal irradiation to condition transplant recipients (Ye et al., 2013; Zhang et al., 2004). Both approaches are highly inflammatory and impair BM function. In addition, *Mx1*-Cre–mediated *Cebpa* deletion rapidly depleted granulocytes, which can activate MPP proliferation (Säwén et al., 2016) and confound functional studies of HSPCs. Our data demonstrate that an inflammatory environment is required to reveal the competitive advantage of *Cebpa*-knockout HSPCs.

Transcriptional analyses revealed that *Cebpa* knockout prevents chronic IL-1β–driven activation of myeloid differentiation, as well as metabolic and proteostatic gene programs important
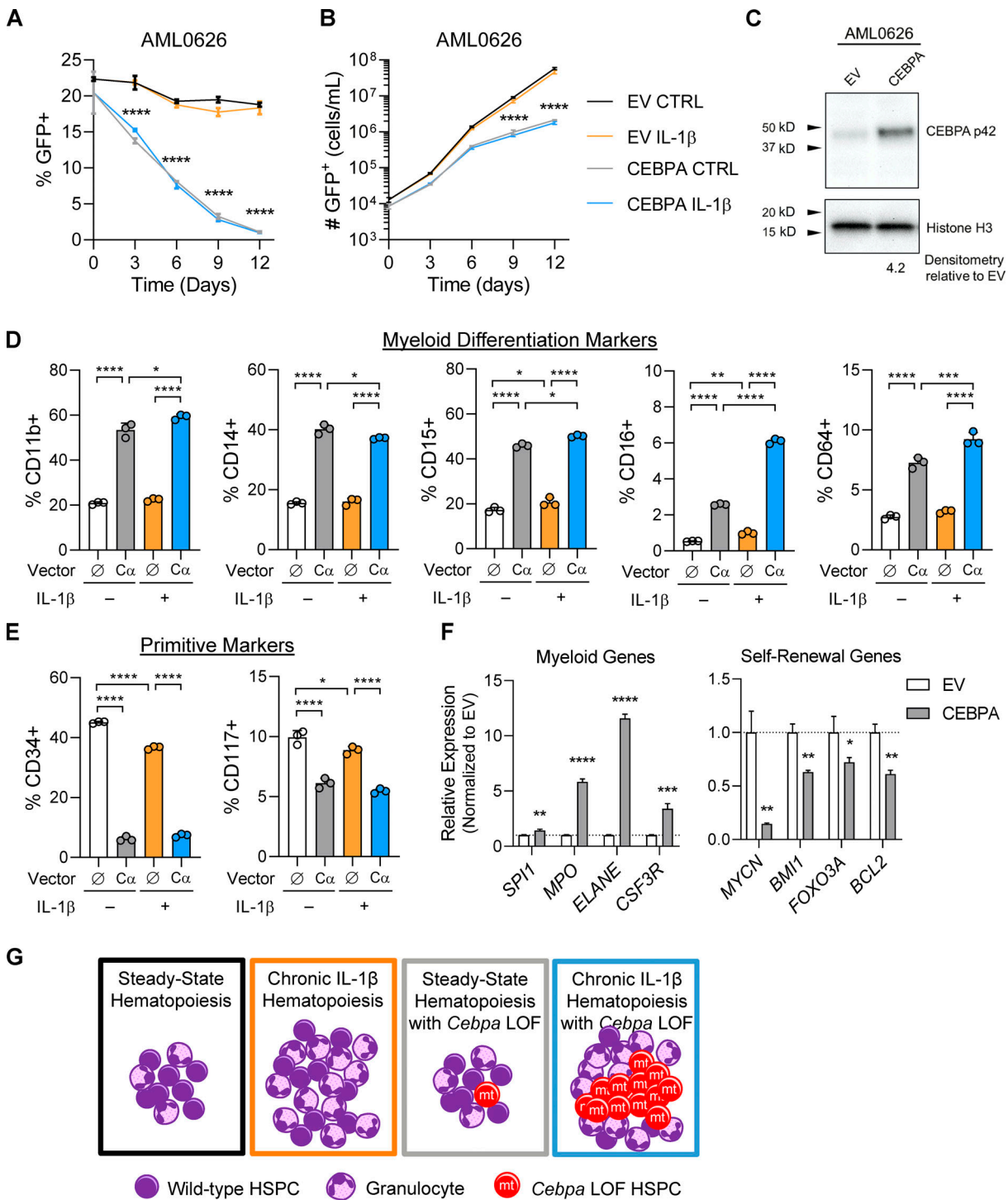
Figure 10. **Ectopic CEBPA expression induces differentiation and impairs fitness in AML cells. (A)** Cell competition dynamics of primary AML sample AML0626 in cell culture. EV, empty vector. **(B)** Cell expansion of primary AML sample AML0626 in cell culture. **(C)** Western blot of sorted GFP⁺ cells at day 6. **(D)** Flow cytometric analysis of differentiation markers on GFP⁺ cells at day 6. **(E)** Flow cytometric analysis of primitive markers on GFP⁺ cells at day 6. **(F)** Gene expression analysis of CEBPA target genes from sorted GFP⁺ cells at day 6. **(G)** Model of inflammation-driven HSPC differentiation that selects for phenotypes such as with *Cebpa* LOF that prevent HSPC differentiation and/or promote self-renewal. For A–F, $n = 3$ per group, presented as mean ± SD, and analyzed by two-way ANOVA with Tukey's multiple comparisons test (A and B, D and E) and unpaired t test (F). *, $P < 0.05$; **, $P < 0.01$; ***, $P < 0.001$; ****, $P < 0.0001$. Data are representative of three experiments.

for differentiation. Despite the preexisting molecular priming of MPP3s toward myeloid lineage differentiation (Cabezas-Wallscheid et al., 2014; Pietras et al., 2015), our data show that chronic IL-1β further activates these pathways, consistent with the capacity of myeloid lineage progenitors to overproduce myeloid cells in response to "emergency" cues (Hérault et al., 2017; Kang et al., 2020; Manz and Boettcher, 2014). The dependence of these gene programs on C/EBPα is consistent with its role as a key master regulator that initiates myeloid lineage priming in the LSK population (Pundhir et al., 2018). It is interesting that chronic IL-1β has been shown to induce precocious myeloid differentiation via PU.1 (Pietras et al., 2016). C/EBPα can regulate PU.1 expression and enhancer binding in preGMs (Pundhir et al., 2018). In fact, PU.1 expression was significantly reduced in *Cebpa*^Δ/Δ MPP3s in the context of chronic IL-1β (Fig. S3 A). Collectively, these data suggest that *Cebpa* is important for GM-lineage specification in MPP3s and that chronic IL-1β primes GM-lineage output via *Cebpa*-dependent gene programs in MPP3s. In addition, *Cebpa* knockout prevents chronic IL-1β–driven repression of stem cell self-renewal genes, *Bmi1*, *Foxo3*, *Mpl*, and *Mycn* (Iwama et al., 2004; Laurenti et al., 2008; Miyamoto et al., 2007; Nitta et al., 2020; Yoshihara et al., 2007), and C/EBPα has been demonstrated to directly bind to the promoters of *Mycn* (Ye et al., 2013) and *Foxo3* (Hasemann et al., 2014). Mining of publicly available ChIP-seq datasets revealed that the *Cebpa*-dependent IL-1β–regulated genes are directly regulated by C/EBPα and/or PU.1, further supporting a model in which C/EBPα integrates inflammatory cues to regulate gene expression programs, either independently or in concert with PU.1.

While steady-state hematopoiesis results in balanced lineage output, chronic IL-1β expands the MPP compartment to increase myeloid output. However, IL-1β–induced differentiation gene programs likely serve as a limiting mechanism that prevents aberrant accumulation of HSPCs. Our data support a model wherein aberrant expansion of HSPCs with *Cebpa* LOF is an emergent property triggered by inflammatory signals such as chronic IL-1β. Our findings suggest that *Cebpa* LOF HSPCs fail to differentiate and instead activate expression of stem cell self-renewal genes, thereby promoting their selective expansion, while WT HSPCs differentiate in response to chronic IL-1β (Fig. 10 G). Still, this selective expansion is reversed upon resolution of inflammation (Fig. 4), suggesting that inflammation must be sufficiently chronic to provide a window of opportunity to favor *Cebpa* LOF and thus leukemia initiation. As such, IL-1β promotion of emergency granulopoiesis, dependent on C/EBPα, is able to play its critical role in host defense (essential for host fitness). These programs carry the risk of promoting leukemogenesis, although this risk is largely relegated to older ages or rare circumstances (evolutionarily, a minor fitness cost). Still, in these contexts, chronic inflammation and its downstream effectors may represent a therapeutic target that could slow leukemogenesis.

Finally, we showed that primitive M0–M2 AML subtypes, relapsed AML, and AML secondary to MDS or MPN were associated with a lower *Cebpa*-dependent IL-1β–regulated gene score, corresponding to greater expression of *Cebpa*-dependent IL-1β–

down-regulated genes (e.g., stemness genes). The *Cebpa*-dependent IL-1β–regulated gene score may provide additional information on the phenotype of an AML and aid in predicting prognosis and therapeutic response in AML. We further show that the maintenance of low CEPBA activity by AMLs is important for their fitness, as ectopic expression of CEBPA conferred a competitive disadvantage on AMLs, coinciding with increased differentiation and reduced expression of stemness genes. AMLs may need to evolve reduced CEPBA activity to convert IL-1β from a negative regulator of HSPC fitness (Pietras et al., 2016; Chavez et al., 2021) into a positive contributor to AML fitness (Carey et al., 2017).

There is growing evidence of context-specific expansion of oncogenically initiated hematopoietic progenitors: *BCR-ABL* or *Ppm1d* deficiency with chemotherapy (Bilousova et al., 2005; Hsu et al., 2018; Kahn et al., 2018); *Notch* activation, *Tp53*-deficiency, or *Cebpa*-deficiency following γ-irradiation (Bondar and Medzhitov, 2010; Fleenor et al., 2015b; Marusyk et al., 2009; Marusyk et al., 2010); BCR-ABL, *Myc*, *NRas*^V12, or AML1-ETO in aging (Henry et al., 2015; Henry et al., 2010; Vas et al., 2012); *Jak*^V617F with TNF-α exposure (Fleischman et al., 2011); *Tet2*-knockout with LPS challenge; microbe-induced inflammation (Cai et al., 2018; Meisel et al., 2018); or *DNMT3A* mutations in the setting of bacteria-induced IFNγ signaling (Hormaechea-Agulla et al., 2021). Here, we show that chronic IL-1β is sufficient to drive selective expansion of *Cebpa*-knockout MPPs, directly connecting an inflammatory signaling pathway to a transcriptional fate network. These findings have important implications for the earliest events that could drive clonal hematopoiesis with indeterminate potential, MDS, MPN, or AML. Initially, IL-1 drives selection for mutations in HSPCs that provide resistance to the prodifferentiative effects of IL-1. This expansion will proportionally increase the odds of successive mutation accumulation in the same clone, increasing the possibility of leukemic transformation. Once transformed, IL-1 can then act as a growth factor for AML blasts (Carey et al., 2017) and contribute to more aggressive disease (Barreyro et al., 2012). Therefore, inflammation could be an important driver of leukemogenesis and could represent a potential target for intervention.

Materials and methods

Mice
Cebpa^loxP/loxP mice (kind gift of Daniel G. Tenen) were previously described (Zhang et al., 2004). *HSC-SCL-Cre-ER*^T transgenic mice were generously provided by Joachim Göthert (Göthert et al., 2005). *R26R-EYFP* transgenic reporter mice were generously provided by Dennis Roop (Srinivas et al., 2001). All mice were backcrossed for at least five generations on a C57BL/6 background and bred to be heterozygous for *R26R-EYFP* and heterozygous for *HSC-SCL-Cre-ER*^T, while each litter contained a mixture of *Cebpa* genotypes, such that *Cebpa*^+/+ and *Cebpa*^Δ/Δ littermates were used in experiments. To induce recombination, mice were treated i.p. with 2.5 mg of tamoxifen (prepared at 10 mg/ml in corn oil) daily for 3 d and were used for experiments 7 d after the final dose of tamoxifen. Genotyping of mice and detection of recombined product were as previously

Higa et al.
Interleukin-1–mediated selection for *Cebpa* loss

Journal of Experimental Medicine
https://doi.org/10.1084/jem.20200560

described (Zhang et al., 2004). C57BL/6 (Ly5.2) and congenic (Ly5.1) mice were ordered from Charles River Laboratories. All procedures were performed in accordance with the University of Colorado Anschutz Medical Campus Institutional Animal Care and Use Committee–approved animal protocols.

Lentiviral vectors
The *CEBPA*-expressing vector was generated by subcloning the full-length ORF (Sino Biological) into the GFP-expressing lentiviral vector pUltra (Addgene). Lentiviral particles where produced by triple transfection of HEK293FT cells with pUltra-*CEBPA*, pSPAX2, and pMD2.G. The supernatant was harvested after 24 h, and the virus was concentrated by ultracentrifugation at 40,000 ×g for 2 h at 4°C over a 20% sucrose cushion. Lentiviral transduction was performed by plating the cells at 500,000–1,000,000/ml with the lentiviral supernatant in the presence of 4 µg/ml polybrene and centrifuging the plate at 1,000 ×g for 1 h at 32°C followed by incubation for 24 h at 37°C, at the end of which the medium was replaced with fresh medium. C/EBPα expression was determined by Western blot.

Cell preparation and flow cytometry
Peripheral blood for flow cytometry analysis or complete blood count was collected in heparin (50 U/ml) from the submandibular vein of live mice or via cardiac puncture from terminal mice. Complete blood count analyses were run on a Heska HT5 blood analyzer. For flow cytometry analyses, RBCs were hemolyzed with ammonium-chloride-potassium (ACK) lysis buffer, and cells were washed and filtered. Cell were stained for mature immune cells using the following antibodies: rat IgG for blocking, Mac1 (M1/70) Brilliant Ultraviolet 395 (BUV395), Gr1 (Rb6-8C5) Pacific Blue, CD45.2 (104) biotin, streptavidin Brilliant Violet (BV) 605, B220 (RA3-6B2) BV786, CD45.1 (A20) PerCP-Cy5.5, CD8 (53-6.7) PE, Ter-119 (TER-119) PE-Cy5, CD4 (GK1.5) PE-Cy7, IgM (RMM-1) APC, CD3 (17A2) Alexa Fluor 700, and CD19 (1D3) APC-Cy7. BM for flow analysis was obtained by flushing cells from one tibia and one femur per mouse. RBCs were hemolyzed with ACK lysis buffer, and cells were washed and filtered. Cell counts were collected on the Guava easyCyte System (Millipore). BM cells were stained for mature immune cells as with peripheral blood and for HSPCs with the following antibodies: rat IgG, Mac1 BUV395, Sca1 (D7) BV421, CD41 (MWReg30) BV510, CD45.2 biotin, streptavidin BV605, CD105 (MJ7/18) BV711, CD150 (TC15-12F12.2) BV785, CD45.1 PerCP-Cy.5.5, Flk2 (A2F10) PE, lineage cocktail (B220, CD3, CD4, CD5 [53-7.3], CD8, Gr1, Ter119) conjugated with PE-Cy5, FcgR (93) PE-Cy7, CD34 (RAM34) eFluor(e)660, CD48 (HM48-1) Alexa Fluor 700, and cKit (2B8) APC-Cy7. Data were collected on the ZE5 cell analyzer (Bio-Rad) or the LSRFortessa (BD Biosciences) and analyzed with FlowJo software v10. BM for cell sorting was obtained by crushing all long bones and spines from each mouse. RBCs were hemolysed with ACK lysis buffer, and cells were washed and filtered. BM cells were lineage depleted using Mouse Lineage Cell Depletion Kit (Miltenyi Biotec). Cells were stained to identify HSPCs with the following antibodies: rat IgG, CD48 e450, CD45.2 biotin, streptavidin BV605, CD150 BV786, CD45.1 PerCP-Cy5.5, Flk2 PE, cKit PE-Cy7, Sca1 APC, and lineage

cocktail conjugated with APC-Cy7. Cell sorting was performed with the 100-µm nozzle on the FACSAria Fusion (BD Biosciences). Flow cytometry analysis was performed on cells from liquid culture and on individual colonies from methylcellulose with the following antibodies: rat IgG, Mac1 BUV395, Gr1 Pacific Blue, Sca1 APC, and cKit PE-Cy7. Data were collected on the ZE5 cell analyzer (Bio-Rad) and analyzed with FlowJo v10. AML cells were immunophenotyped with the following antibodies: CD11b BUV395, CD117 BV421, CD64 BV510, CD16 BV605, CD38 PE, CD15 PE-Cy5, CD45 PE-Cy7, CD34 APC, and CD14 APC-Cy7, and analyzed on the LSRFortessa (BD Biosciences; van Lochem et al., 2004).

Cell culture
For liquid cultures of murine primary cells, 200 YFP⁺ LSK cells were sorted from *Cebpa*^+/+ or *Cebpa*^Δ/Δ mice into wells of a 96-well culture plate. Cells were grown in IMDM (Gibco) with 20% heat-inactivated FBS (HyClone), 50 µM β-mercaptoethanol, 100 ng/ml mIL-6, 100 ng/ml mFlt3-ligand, 100 ng/ml murine stem cell factor (SCF), and 10 ng/ml IL-11, as previously described (Varnum-Finney et al., 2003). For CFU assays, 100 YFP⁺ LSK cells were sorted from *Cebpa*^+/+ or *Cebpa*^Δ/Δ mice and plated in methylcellulose (HSC006; R&D Systems; 1 ml in 3-cm dish) containing IMDM, antibiotic-antimycotic (Gibco), 25 ng/ml SCF, 25 ng/ml Flt3-liter, 25 ng/ml IL-11, 10 ng/ml IL-3, 10 ng/ml GM-CSF, 25 ng/ml thrombopoietin, and 4 U/ml erythropoietin with or without 25 ng/ml IL-1β. Colonies were counted and scored under a dissecting scope after 7 d. For serial replating, 10^4 cells were replated in fresh methylcellulose with or without IL-1β. All cytokines were obtained from Peprotech. We calculated cumulative CFU potential with the following equation:

$$\frac{\text{CFU replating}}{\text{number of cells replated}} \times \text{number of cell from initial plating.}$$

AML cell lines MOLM-13, MOLM-14, and EOL-1 and CML cell line K562 were maintained in IMDM with 2 mM glutamine, 10% heat-inactivated FBS, and 100 U/ml penicillin/streptomycin. Primary AML sample AML0626 (derived from a relapsed patient, FAB = M0/1/2, with *IDH1*-R132 and *KIT*-D816V mutations) was generously provided by Craig Jordan (University of Colorado Anschutz Medical Campus, Aurora, CO) and was maintained in IMDM, 20% BSA, insulin, and transferrin (BIT; Stem Cell Technologies), LDL 1:300 (Calbiochem), 50 µM β-mercaptoethanol, 100 U/ml penicillin/streptomycin, 10 ng/ml SCF 10 ng/ml, 10 ng/ml IL-3, and 10 ng/ml FLT3L. For AML cell competition assays, cells were transduced with the empty vector or *CEBPA*-expressing vector and then mixed with nontransduced cells to obtain a population containing ~25% GFP⁺ cells. MOLM13, MOLM14, and EOL-1 were plated at 100,000 cells/ml, K562 were plated at 50,000 cells/ml, and AML0626 were plated at 200,000 cells/ml with or without 25 ng/ml IL-1β. Every 3 d, cells were counted, the percentage of GFP⁺ cells was tested with the Guava easyCyte flow cytometer (Millipore), and cells were replated at the same initial density.

Competitive transplants

To obtain a starting donor chimerism of ~5%, 2×10^3 LSK cells were sorted and transplanted with 2×10^6 competitor whole BM cells into mildly conditioned congenic mice. Mild conditioning was achieved by treating mice with 20 mg/kg of busulfan 4 d before transplant and 30 µg of anti-CD4 antibody, clone GK1.5 (BioXcell), and 30 µg of anti-CD8 antibody, clone 2.43 (Bio-X-Cell), 2 d before transplant. Busulfan was prepared fresh at 20 mg/ml in DMSO and diluted in saline to 2 mg/ml, while kept warm and protected from light. CD4 and CD8 T cell–depleting antibodies were prepared at 30 µg per 0.1 ml of PBS. Initial chimerism was assessed 3 wk after transplant, and mice were subsequently treated daily for 20 d with 0.1% BSA/PBS or 0.5 µg IL-1β (Peprotech) in 0.1% BSA/PBS via i.p. injection.

Fluidigm Biomark gene expression analysis

Cells were cultured for 12 h as described above. Live cells were subsequently sorted to purity into 96-well plates at 50 cells/well in 5 µl CellsDirect 2× Reaction Buffer (Invitrogen). A panel of 96 target genes were preamplified for 20 rounds with Superscript III (Invitrogen) using a custom-designed set of target-specific primers. Preamplified cDNA was treated with Exonuclease I (New England Biolabs) to remove excess primers, diluted in DNA suspension buffer (Clontech), loaded with custom-designed primer sets onto a Fluidigm 96.96 DynamicArray IFC, and run on a BioMark HD System (Fluidigm) using SsoFast Sybr Green for detection (Bio-Rad). Data were analyzed by the cycle threshold (ΔΔCt) method using Fluidigm software, and gene expression values were normalized to *Gusb* expression.

RNA-seq

Cells were sorted directly into RLT Buffer, and RNA was extracted using RNeasy Micro Kit (Qiagen). Library construction was performed using the SMARTer Stranded Total RNA-Seq Kit v2, Pico Input Mammalian (Takara), and paired-end sequencing was performed on the NovaSeq 6000 instrument (Illumina) by the University of Colorado Cancer Center Genomics Shared Resource. Illumina adapters were removed using BBDuk (Bushnell, 2019), and reads <50 bp after trimming were discarded. Reads were aligned and quantified using STAR v2.6.0a (Dobin et al., 2013) to the Ensembl mouse transcriptome (GRCm38.p6, release 96). Normalization and differential expression were calculated using the limma R package (Ritchie et al., 2015). Differentially expressed genes (adjusted P < 0.05) comparing the donors of group C versus the donors of group A were determined to be influenced by IL-1β (Fig. 3 A). These genes were further determined to be *Cebpa* dependent or independent based on whether they were significantly altered when comparing the donors of group D to the donors of group B. ORA was performed on these genes using the ClusterProfiler R package (Yu et al., 2012) with Hallmark and GO Biological Processes gene sets from the Molecular Signatures Database (Liberzon et al., 2011), along with select published gene sets (Cabezas-Wallscheid et al., 2014; Chambers et al., 2007; Giladi et al., 2018; Ye et al., 2013). GSEA was performed on the fold change of the genes for each comparison using the fGSEA R package with 10,000 permutations (Sergushichev, 2016 *Preprint*)

with the same gene sets. Heatmaps were generated with the ComplexHeatmap R package (Gu et al., 2016) following z-score transformation. The genes in the pathway heatmaps were selected because of their presence in the leading edge as determined by fGSEA for the indicated comparison. Raw and processed RNA-seq data are deposited in GEO under accession no. GSE166629 (Edgar et al., 2002).

Cell cycle analysis

Cells were sorted and fixed into FACS buffer, and then immediately fixed in BD Cytofix/Cytoperm. Cells were restained with surface stain, and intracellular staining for Ki67 (SolA15) APC was performed with the Fixation/Permeabilization Solution Kit (BD Bioscience) and as previously described (Jalbert and Pietras, 2018). Data were collected on the ZE5 cell analyzer (Bio-Rad) and analyzed with FlowJo v10.

RNA-seq data mining

The fgsea R package was used to conduct pathway analysis on the effect of in vitro radiation in LSK (GEO accession no. GSE61602; Fleenor et al., 2015b).

ChIP-seq data mining

C/EBPα and PU.1 ChIP binding data in LSK, preGM, GMP, and granulocytes were downloaded from GEO (accession no. GSE89767; Pundhir et al., 2018). The clusterProfiler R package was used to determine the enrichment between *Cebpa*-dependent IL1 up- and down-regulated genes and the genes in each binding category.

AML data mining

TCGA AML (Firehose Legacy; Ley et al., 2013) transcripts per million–normalized and Tyner AML (Tyner et al., 2018) counts per million–normalized gene expression data were downloaded from cBioPortal on June 19, 2020 (Cerami et al., 2012). Genes with mean transcripts per million <1 in the TCGA were removed. The genes of each dataset were z-score transformed and separated into *Cebpa*-dependent IL1 up- and down-regulated genes. The difference in the sample sum of z-scores for each gene grouping was calculated and subsequently z-score transformed. A higher signature score corresponds to greater similarity to the Cebpa-dependent changes observed upon IL-1 treatment.

Statistics

Unpaired Mann-Whitney *U* test or unpaired Student's *t*-test (for bivariate comparison) or two-way ANOVA with Tukey's multiple comparisons test (for multivariate comparison) was performed in Prism software v8 (GraphPad); *, P < 0.05; **, P < 0.01; ***, P < 0.001; and ****, P < 0.0001.

Online supplemental material

Fig. S1 shows characterization of primary *Cebpa*-knockout mice. Fig. S2 shows supporting analyses of competitive transplants. Fig. S3 shows that *Cebpa* knockout is epistatic to chronic IL-1β, by preventing up-regulation of myeloid differentiation programs and down-regulation of stem gene programs, and that gene expression of competitors is affected by the donor genotype

they were competed against. Fig. S4 shows supporting MPP3 cell culture data and cell competition in AML cell lines. Table S1 lists genes from heatmaps presented in Figs. 5 B, 6 C, 7 C, and S3 B.

Author contributions: K.C. Higa performed all experiments with assistance from J.S. Chavez, V. Zaberezhnyy, J.L. Rabe, M. De Dominici, and E.M. Pietras. K.C. Higa, A. Goodspeed, and E.P. Danis performed bioinformatic analyses. D.G. Tenen provided resources and interpreted results. K.C. Higa, E.M. Pietras, and J. DeGregori designed research studies, interpreted results, and wrote the manuscript.

Disclosures: The authors declare no competing interests exist.

References

Barreyro, L., B. Will, B. Bartholdy, L. Zhou, T.I. Todorova, R.F. Stanley, S. Ben-Neriah, C. Montagna, S. Parekh, A. Pellagatti, et al. 2012. Overexpression of IL-1 receptor accessory protein in stem and progenitor cells and outcome correlation in AML and MDS. *Blood*. 120:1290–1298. https://doi.org/10.1182/blood-2012-01-404699

Bennett, J.M., D. Catovsky, M.T. Daniel, G. Flandrin, D.A. Galton, H.R. Gralnick, and C. Sultan. 1985. Proposed revised criteria for the classification of acute myeloid leukemia. A report of the French-American-British Cooperative Group. *Ann. Intern. Med.* 103:620–625. https://doi.org/10.7326/0003-4819-103-4-620

Bereshchenko, O., E. Mancini, S. Moore, D. Bilbao, R. Månsson, S. Luc, A. Grover, S.E. Jacobsen, D. Bryder, and C. Nerlov. 2009. Hematopoietic stem cell expansion precedes the generation of committed myeloid leukemia-initiating cells in C/EBPalpha mutant AML. *Cancer Cell.* 16:390–400. https://doi.org/10.1016/j.ccr.2009.09.036

Bilousova, G., A. Marusyk, C.C. Porter, R.D. Cardiff, and J. DeGregori. 2005. Impaired DNA replication within progenitor cell pools promotes leukemogenesis. *PLoS Biol.* 3:e401. https://doi.org/10.1371/journal.pbio.0030401

Bondar, T., and R. Medzhitov. 2010. p53-mediated hematopoietic stem and progenitor cell competition. *Cell Stem Cell.* 6:309–322. https://doi.org/10.1016/j.stem.2010.03.002

Bowling, S., K. Lawlor, and T.A. Rodríguez. 2019. Cell competition: the winners and losers of fitness selection. *Development.* 146:dev167486. https://doi.org/10.1242/dev.167486

Bowman, R.L., L. Busque, and R.L. Levine. 2018. Clonal hematopoiesis and evolution to hematopoietic malignances. *Cell Stem Cell.* 22:157–170. https://doi.org/10.1016/j.stem.2018.01.011

Busch, K., K. Klapproth, M. Barile, M. Flossdorf, T. Holland-Letz, S.M. Schlenner, M. Reth, T. Höfer, and H.R. Rodewald. 2015. Fundamental properties of unperturbed haematopoiesis from stem cells in vivo. *Nature.* 518:542–546. https://doi.org/10.1038/nature14242

Bushnell, B. 2019. BBTools:BBMap. https://sourceforge.net/projects/bbmap/

Cabezas-Wallscheid, N., D. Klimmeck, J. Hansson, D.B. Lipka, A. Reyes, Q. Wang, D. Weichenhan, A. Lier, L. von Paleske, S. Renders, et al. 2014. Identification of regulatory networks in HSCs and their immediate progeny via integrated proteome, transcriptome, and DNA methylome analysis. *Cell Stem Cell.* 15:507–522. https://doi.org/10.1016/j.stem.2014.07.005

Cai, Z., J.J. Kotzin, B. Ramdas, S. Chen, S. Nelanuthala, L.R. Palam, R. Pandey, R.S. Mali, Y. Liu, M.R. Kelley, et al. 2018. Inhibition of inflammatory signaling in Tet2 mutant preleukemic cells mitigates stress-induced abnormalities and clonal hematopoiesis. *Cell Stem Cell.* 23:833–849.e5. https://doi.org/10.1016/j.stem.2018.10.013

Carey, A., D.K. Edwards V, C.A. Eide, L. Newell, E. Traer, B.C. Medeiros, D.A. Pollyea, M.W. Deininger, R.H. Collins, J.W. Tyner, et al. 2017. Identification of interleukin-1 by functional screening as a key mediator of cellular expansion and disease progression in acute myeloid leukemia. *Cell Rep.* 18:3204–3218. https://doi.org/10.1016/j.celrep.2017.03.018

Cerami, E., J. Gao, U. Dogrusoz, B.E. Gross, S.O. Sumer, B.A. Aksoy, A. Jacobsen, C.J. Byrne, M.L. Heuer, E. Larsson, et al. 2012. The cBio cancer genomics portal: an open platform for exploring multidimensional cancer genomics data. *Cancer Discov.* 2:401–404. https://doi.org/10.1158/2159-8290.CD-12-0095

Chambers, S.M., N.C. Boles, K.Y. Lin, M.P. Tierney, T.V. Bowman, S.B. Bradfute, A.J. Chen, A.A. Merchant, O. Sirin, D.C. Weksberg, et al. 2007. Hematopoietic fingerprints: an expression database of stem cells and their progeny. *Cell Stem Cell.* 1:578–591. https://doi.org/10.1016/j.stem.2007.10.003

Chavez, J.S., J.L. Rabe, D. Loeffler, K.C. Higa, G. Hernandez, T.S. Mills, N. Ahmed, R.L. Gessner, Z. Ke, B.M. Idler, et al. 2021. PU.1 enforces quiescence and limits hematopoietic stem cell expansion during inflammatory stress. *J. Exp. Med.* 218:e20201169. https://doi.org/10.1084/jem.20201169

Corces, M.R., H.Y. Chang, and R. Majeti. 2017. Preleukemic hematopoietic stem cells in human acute myeloid leukemia. *Front. Oncol.* 7:263. https://doi.org/10.3389/fonc.2017.00263

Dobin, A., C.A. Davis, F. Schlesinger, J. Drenkow, C. Zaleski, S. Jha, P. Batut, M. Chaisson, and T.R. Gingeras. 2013. STAR: Ultrafast universal RNA-seq aligner. *Bioinformatics.* 29:15–21. https://doi.org/10.1093/bioinformatics/bts635

Dufour, A., F. Schneider, E. Hoster, T. Benthaus, B. Ksienzyk, S. Schneider, P.M. Kakadia, M.C. Sauerland, W.E. Berdel, T. Büchner, et al. AML CG study group. 2012. Monoallelic CEBPA mutations in normal karyotype acute myeloid leukemia: independent favorable prognostic factor within NPM1 mutated patients. *Ann. Hematol.* 91:1051–1063. https://doi.org/10.1007/s00277-012-1423-4

Edgar, R., M. Domrachev, and A.E. Lash. 2002. Gene Expression Omnibus: NCBI gene expression and hybridization array data repository. *Nucleic Acids Res.* 30:207–210. https://doi.org/10.1093/nar/30.1.207

Ernst, T., A. Chase, K. Zoi, K. Waghorn, C. Hidalgo-Curtis, J. Score, A. Jones, F. Grand, A. Reiter, A. Hochhaus, and N.C. Cross. 2010. Transcription factor mutations in myelodysplastic/myeloproliferative neoplasms. *Haematologica.* 95:1473–1480. https://doi.org/10.3324/haematol.2010.021808

Fleenor, C.J., K. Higa, M.M. Weil, and J. DeGregori. 2015a. Evolved cellular mechanisms to respond to genotoxic insults: Implications for radiation-induced hematologic malignancies. *Radiat. Res.* 184:341–351. https://doi.org/10.1667/RR14147.1

Fleenor, C.J., A.I. Rozhok, V. Zaberezhnyy, D. Mathew, J. Kim, A.C. Tan, I.D. Bernstein, and J. DeGregori. 2015b. Contrasting roles for C/EBPα and Notch in irradiation-induced multipotent hematopoietic progenitor cell defects. *Stem Cells.* 33:1345–1358. https://doi.org/10.1002/stem.1936

Fleischman, A.G., K.J. Aichberger, S.B. Luty, T.G. Bumm, C.L. Petersen, S. Doratotaj, K.B. Vasudevan, D.H. LaTocha, F. Yang, R.D. Press, et al. 2011.

TNFα facilitates clonal expansion of JAK2V617F positive cells in myeloproliferative neoplasms. *Blood.* 118:6392–6398. https://doi.org/10.1182/blood-2011-04-348144

Gan, B., and R.A. DePinho. 2009. mTORC1 signaling governs hematopoietic stem cell quiescence. *Cell Cycle.* 8:1003–1006. https://doi.org/10.4161/cc.8.7.8045

García-Prat, L., P. Sousa-Victor, and P. Muñoz-Cánoves. 2017. Proteostatic and metabolic control of stemness. *Cell Stem Cell.* 20:593–608. https://doi.org/10.1016/j.stem.2017.04.011

Ghandi, M., F.W. Huang, J. Jané-Valbuena, G.V. Kryukov, C.C. Lo, E.R. McDonald III, J. Barretina, E.T. Gelfand, C.M. Bielski, H. Li, et al. 2019. Next-generation characterization of the Cancer Cell Line Encyclopedia. *Nature.* 569:503–508. https://doi.org/10.1038/s41586-019-1186-3

Giladi, A., F. Paul, Y. Herzog, Y. Lubling, A. Weiner, I. Yofe, D. Jaitin, N. Cabezas-Wallscheid, R. Dress, F. Ginhoux, et al. 2018. Single-cell characterization of haematopoietic progenitors and their trajectories in homeostasis and perturbed haematopoiesis. *Nat. Cell Biol.* 20:836–846. https://doi.org/10.1038/s41556-018-0121-4

Göthert, J.R., S.E. Gustin, M.A. Hall, A.R. Green, B. Göttgens, D.J. Izon, and C.G. Begley. 2005. In vivo fate-tracing studies using the Scl stem cell enhancer: embryonic hematopoietic stem cells significantly contribute to adult hematopoiesis. *Blood.* 105:2724–2732. https://doi.org/10.1182/blood-2004-08-3037

Green, C.L., K.K. Koo, R.K. Hills, A.K. Burnett, D.C. Linch, and R.E. Gale. 2010. Prognostic significance of CEBPA mutations in a large cohort of younger adult patients with acute myeloid leukemia: impact of double CEBPA mutations and the interaction with FLT3 and NPM1 mutations. *J. Clin. Oncol.* 28:2739–2747. https://doi.org/10.1200/JCO.2009.26.2501

Gu, X., Q. Ebrahem, R.Z. Mahfouz, M. Hasipek, F. Enane, T. Radivoyevitch, N. Rapin, B. Przychodzen, Z. Hu, R. Balusu, et al. 2018. Leukemogenic nucleophosmin mutation disrupts the transcription factor hub that regulates granulomonocytic fates. *J. Clin. Invest.* 128:4260–4279. https://doi.org/10.1172/JCI97117

Gu, Z., R. Eils, and M. Schlesner. 2016. Complex heatmaps reveal patterns and correlations in multidimensional genomic data. *Bioinformatics.* 32:2847–2849. https://doi.org/10.1093/bioinformatics/btw313

Guo, H., O. Ma, N.A. Speck, and A.D. Friedman. 2012. Runx1 deletion or dominant inhibition reduces Cebpa transcription via conserved promoter and distal enhancer sites to favor monopoiesis over granulopoiesis. *Blood.* 119:4408–4418. https://doi.org/10.1182/blood-2011-12-397091

Hasemann, M.S., F.K. Lauridsen, J. Waage, J.S. Jakobsen, A.K. Frank, M.B. Schuster, N. Rapin, F.O. Bagger, P.S. Hoppe, T. Schroeder, and B.T. Porse. 2014. C/EBPα is required for long-term self-renewal and lineage priming of hematopoietic stem cells and for the maintenance of epigenetic configurations in multipotent progenitors. *PLoS Genet.* 10: e1004079. https://doi.org/10.1371/journal.pgen.1004079

Henry, C.J., M. Casás-Selves, J. Kim, V. Zaberezhnyy, L. Aghili, A.E. Daniel, L. Jimenez, T. Azam, E.N. McNamee, E.T. Clambey, et al. 2015. Aging-associated inflammation promotes selection for adaptive oncogenic events in B cell progenitors. *J. Clin. Invest.* 125:4666–4680. https://doi.org/10.1172/JCI83024

Henry, C.J., A. Marusyk, V. Zaberezhnyy, B. Adane, and J. DeGregori. 2010. Declining lymphoid progenitor fitness promotes aging-associated leukemogenesis. *Proc. Natl. Acad. Sci. USA.* 107:21713–21718. https://doi.org/10.1073/pnas.1005486107

Hérault, A., M. Binnewies, S. Leong, F.J. Calero-Nieto, S.Y. Zhang, Y.A. Kang, X. Wang, E.M. Pietras, S.H. Chu, K. Barry-Holson, et al. 2017. Myeloid progenitor cluster formation drives emergency and leukaemic myelopoiesis. *Nature.* 544:53–58. https://doi.org/10.1038/nature21693

Ho, T.C., M. LaMere, B.M. Stevens, J.M. Ashton, J.R. Myers, K.M. O'Dwyer, J.L. Liesveld, J.H. Mendler, M. Guzman, J.D. Morrissette, et al. 2016. Evolution of acute myelogenous leukemia stem cell properties after treatment and progression. *Blood.* 128:1671–1678. https://doi.org/10.1182/blood-2016-02-695312

Hormaechea-Agulla, D., K.A. Matatall, D.T. Le, B. Kain, X. Long, P. Kus, R. Jaksik, G.A. Challen, M. Kimmel, and K.Y. King. 2021. Chronic infection drives Dnmt3a-loss-of-function clonal hematopoiesis via IFNγ signaling. *Cell Stem Cell.*:S1934-5909(21)00108-9. https://doi.org/10.1016/j.stem.2021.03.002

Hsu, J.I., T. Dayaram, A. Tovy, E. De Braekeleer, M. Jeong, F. Wang, J. Zhang, T.P. Heffernan, S. Gera, J.J. Kovacs, et al. 2018. PPM1D mutations drive clonal hematopoiesis in response to cytotoxic chemotherapy. *Cell Stem Cell.* 23:700–713.e6. https://doi.org/10.1016/j.stem.2018.10.004

Ito, K., and T. Suda. 2014. Metabolic requirements for the maintenance of self-renewing stem cells. *Nat. Rev. Mol. Cell Biol.* 15:243–256. https://doi.org/10.1038/nrm3772

Iwama, A., H. Oguro, M. Negishi, Y. Kato, Y. Morita, H. Tsukui, H. Ema, T. Kamijo, Y. Katoh-Fukui, H. Koseki, et al. 2004. Enhanced self-renewal of hematopoietic stem cells mediated by the polycomb gene product Bmi-1. *Immunity.* 21:843–851. https://doi.org/10.1016/j.immuni.2004.11.004

Jalbert, E., and E.M. Pietras. 2018. Analysis of Murine Hematopoietic Stem Cell Proliferation During Inflammation. *In* Cellular Quiescence: Methods and Protocols. H.D. Lacorazza, editor. Springer New York, New York, NY. pp. 183–200. https://doi.org/10.1007/978-1-4939-7371-2_14

Johnson, P.F. 2005. Molecular stop signs: regulation of cell-cycle arrest by C/EBP transcription factors. *J. Cell Sci.* 118:2545–2555. https://doi.org/10.1242/jcs.02459

Kahn, J.D., P.G. Miller, A.J. Silver, R.S. Sellar, S. Bhatt, C. Gibson, M. McConkey, D. Adams, B. Mar, P. Mertins, et al. 2018. *PPM1D*-truncating mutations confer resistance to chemotherapy and sensitivity to PPM1D inhibition in hematopoietic cells. *Blood.* 132:1095–1105. https://doi.org/10.1182/blood-2018-05-850339

Kang, Y.A., E.M. Pietras, and E. Passegué. 2020. Deregulated Notch and Wnt signaling activates early-stage myeloid regeneration pathways in leukemia. *J. Exp. Med.* 217:e20190787. https://doi.org/10.1084/jem.20190787

Kelly, L.M., and D.G. Gilliland. 2002. Genetics of myeloid leukemias. *Annu. Rev. Genomics Hum. Genet.* 3:179–198. https://doi.org/10.1146/annurev.genom.3.032802.115046

Kirstetter, P., M.B. Schuster, O. Bereshchenko, S. Moore, H. Dvinge, E. Kurz, K. Theilgaard-Mönch, R. Månsson, T.A. Pedersen, T. Pabst, et al. 2008. Modeling of C/EBPalpha mutant acute myeloid leukemia reveals a common expression signature of committed myeloid leukemia-initiating cells. *Cancer Cell.* 13:299–310. https://doi.org/10.1016/j.ccr.2008.02.008

Laurenti, E., B. Varnum-Finney, A. Wilson, I. Ferrero, W.E. Blanco-Bose, A. Ehninger, P.S. Knoepfler, P.F. Cheng, H.R. MacDonald, R.N. Eisenman, et al. 2008. Hematopoietic stem cell function and survival depend on c-Myc and N-Myc activity. *Cell Stem Cell.* 3:611–624. https://doi.org/10.1016/j.stem.2008.09.005

Ley, T.J., C. Miller, L. Ding, B.J. Raphael, A.J. Mungall, A. Robertson, K. Hoadley, T.J. Triche Jr., P.W. Laird, J.D. Baty, et al. Cancer Genome Atlas Research Network. 2013. Genomic and epigenomic landscapes of adult de novo acute myeloid leukemia. *N. Engl. J. Med.* 368:2059–2074. https://doi.org/10.1056/NEJMoa1301689

Liberzon, A., A. Subramanian, R. Pinchback, H. Thorvaldsdóttir, P. Tamayo, and J.P. Mesirov. 2011. Molecular signatures database (MSigDB) 3.0. *Bioinformatics.* 27:1739–1740. https://doi.org/10.1093/bioinformatics/btr260

Loke, J., P.S. Chin, P. Keane, A. Pickin, S.A. Assi, A. Ptasinska, M.R. Imperato, P.N. Cockerill, and C. Bonifer. 2018. C/EBPα overrides epigenetic reprogramming by oncogenic transcription factors in acute myeloid leukemia. *Blood Adv.* 2:271–284. https://doi.org/10.1182/bloodadvances.2017012781

Mantovani, A., C.A. Dinarello, M. Molgora, and C. Garlanda. 2019. Interleukin-1 and related cytokines in the regulation of inflammation and immunity. *Immunity.* 50:778–795. https://doi.org/10.1016/j.immuni.2019.03.012

Manz, M.G., and S. Boettcher. 2014. Emergency granulopoiesis. *Nat. Rev. Immunol.* 14:302–314. https://doi.org/10.1038/nri3660

Marusyk, A., M. Casás-Selves, C.J. Henry, V. Zaberezhnyy, J. Klawitter, U. Christians, and J. DeGregori. 2009. Irradiation alters selection for oncogenic mutations in hematopoietic progenitors. *Cancer Res.* 69: 7262–7269. https://doi.org/10.1158/0008-5472.CAN-09-0604

Marusyk, A., C.C. Porter, V. Zaberezhnyy, and J. DeGregori. 2010. Irradiation selects for p53-deficient hematopoietic progenitors. *PLoS Biol.* 8: e1000324. https://doi.org/10.1371/journal.pbio.1000324

Matatall, K.A., M. Jeong, S. Chen, D. Sun, F. Chen, Q. Mo, M. Kimmel, and K.Y. King. 2016. Chronic infection depletes hematopoietic stem cells through stress-induced terminal differentiation. *Cell Rep.* 17:2584–2595. https://doi.org/10.1016/j.celrep.2016.11.031

Matsuo, Y., R.A. MacLeod, C.C. Uphoff, H.G. Drexler, C. Nishizaki, Y. Katayama, G. Kimura, N. Fujii, E. Omoto, M. Harada, and K. Orita. 1997. Two acute monocytic leukemia (AML-M5a) cell lines (MOLM-13 and MOLM-14) with interclonal phenotypic heterogeneity showing MLL-AF9 fusion resulting from an occult chromosome insertion, ins(11; 9)(q23;p22p23). *Leukemia.* 11:1469–1477.

Meisel, M., R. Hinterleitner, A. Pacis, L. Chen, Z.M. Earley, T. Mayassi, J.F. Pierre, J.D. Ernest, H.J. Galipeau, N. Thuille, et al. 2018. Microbial signals drive pre-leukaemic myeloproliferation in a Tet2-deficient host. *Nature.* 557:580–584. https://doi.org/10.1038/s41586-018-0125-z

Mejia-Ramirez, E., and M.C. Florian. 2020. Understanding intrinsic hematopoietic stem cell aging. *Haematologica.* 105:22–37. https://doi.org/10.3324/haematol.2018.211342

Miyamoto, K., K.Y. Araki, K. Naka, F. Arai, K. Takubo, S. Yamazaki, S. Matsuoka, T. Miyamoto, K. Ito, M. Ohmura, et al. 2007. Foxo3a is essential for maintenance of the hematopoietic stem cell pool. *Cell Stem Cell.* 1:101–112. https://doi.org/10.1016/j.stem.2007.02.001

Nitta, E., N. Itokawa, S. Yabata, S. Koide, L.B. Hou, M. Oshima, K. Aoyama, A. Saraya, and A. Iwama. 2020. Bmi1 counteracts hematopoietic stem cell aging by repressing target genes and enforcing the stem cell gene signature. *Biochem. Biophys. Res. Commun.* 521:612–619. https://doi.org/10.1016/j.bbrc.2019.10.153

Pabst, T., B.U. Mueller, N. Harakawa, C. Schoch, T. Haferlach, G. Behre, W. Hiddemann, D.-E. Zhang, and D.G. Tenen. 2001a. AML1-ETO downregulates the granulocytic differentiation factor C/EBPalpha in t(8;21) myeloid leukemia. *Nat. Med.* 7:444–451. https://doi.org/10.1038/86515

Pabst, T., B.U. Mueller, P. Zhang, H.S. Radomska, S. Narravula, S. Schnittger, G. Behre, W. Hiddemann, and D.G. Tenen. 2001b. Dominant-negative mutations of CEBPA, encoding CCAAT/enhancer binding protein-α (C/EBPalpha), in acute myeloid leukemia. *Nat. Genet.* 27:263–270. https://doi.org/10.1038/85820

Peng, H., A. Kasada, M. Ueno, T. Hoshii, Y. Tadokoro, N. Nomura, C. Ito, Y. Takase, H.T. Vu, M. Kobayashi, et al. 2018. Distinct roles of Rheb and Raptor in activating mTOR complex 1 for the self-renewal of hematopoietic stem cells. *Biochem. Biophys. Res. Commun.* 495:1129–1135. https://doi.org/10.1016/j.bbrc.2017.11.140

Perrotti, D., V. Cesi, R. Trotta, C. Guerzoni, G. Santilli, K. Campbell, A. Iervolino, F. Condorelli, C. Gambacorti-Passerini, M.A. Caligiuri, and B. Calabretta. 2002. BCR-ABL suppresses C/EBPalpha expression through inhibitory action of hnRNP E2. *Nat. Genet.* 30:48–58. https://doi.org/10.1038/ng791

Pietras, E.M. 2017. Inflammation: a key regulator of hematopoietic stem cell fate in health and disease. *Blood.* 130:1693–1698. https://doi.org/10.1182/blood-2017-06-780882

Pietras, E.M., C. Mirantes-Barbeito, S. Fong, D. Loeffler, L.V. Kovtonyuk, S. Zhang, R. Lakshminarasimhan, C.P. Chin, J.M. Techner, B. Will, et al. 2016. Chronic interleukin-1 exposure drives haematopoietic stem cells towards precocious myeloid differentiation at the expense of self-renewal. *Nat. Cell Biol.* 18:607–618. https://doi.org/10.1038/ncb3346

Pietras, E.M., D. Reynaud, Y.A. Kang, D. Carlin, F.J. Calero-Nieto, A.D. Leavitt, J.M. Stuart, B. Göttgens, and E. Passegué. 2015. Functionally distinct subsets of lineage-biased multipotent progenitors control blood production in normal and regenerative conditions. *Cell Stem Cell.* 17:35–46. https://doi.org/10.1016/j.stem.2015.05.003

Porse, B.T., D. Bryder, K. Theilgaard-Mönch, M.S. Hasemann, K. Anderson, I. Damgaard, S.E. Jacobsen, and C. Nerlov. 2005. Loss of C/EBP alpha cell cycle control increases myeloid progenitor proliferation and transforms the neutrophil granulocyte lineage. *J. Exp. Med.* 202:85–96. https://doi.org/10.1084/jem.20050067

Pundhir, S., F.K. Bratt Lauridsen, M.B. Schuster, J.S. Jakobsen, Y. Ge, E.M. Schoof, N. Rapin, J. Waage, M.S. Hasemann, and B.T. Porse. 2018. Enhancer and transcription factor dynamics during myeloid differentiation reveal an early differentiation block in Cebpa null progenitors. *Cell Rep.* 23:2744–2757. https://doi.org/10.1016/j.celrep.2018.05.012

Radomska, H.S., C.S. Huettner, P. Zhang, T. Cheng, D.T. Scadden, and D.G. Tenen. 1998. CCAAT/enhancer binding protein alpha is a regulatory switch sufficient for induction of granulocytic development from bipotential myeloid progenitors. *Mol. Cell. Biol.* 18:4301–4314. https://doi.org/10.1128/MCB.18.7.4301

Ritchie, M.E., B. Phipson, D. Wu, Y. Hu, C.W. Law, W. Shi, and G.K. Smyth. 2015. limma powers differential expression analyses for RNA-sequencing and microarray studies. *Nucleic Acids Res.* 43:e47. https://doi.org/10.1093/nar/gkv007

Säwén, P., S. Lang, P. Mandal, D.J. Rossi, S. Soneji, and D. Bryder. 2016. Mitotic history reveals distinct stem cell populations and their contributions to hematopoiesis. *Cell Rep.* 14:2809–2818. https://doi.org/10.1016/j.celrep.2016.02.073

Sergushichev, A.A. 2016. An algorithm for fast preranked gene set enrichment analysis using cumulative statistic calculation. *BioRxiv.* (Preprint posted June 20, 2016.)

Signer, R.A., J.A. Magee, A. Salic, and S.J. Morrison. 2014. Haematopoietic stem cells require a highly regulated protein synthesis rate. *Nature.* 509:49–54. https://doi.org/10.1038/nature13035

Srinivas, S., T. Watanabe, C.-S. Lin, C.M. William, Y. Tanabe, T.M. Jessell, and F. Costantini. 2001. Cre reporter strains produced by targeted insertion of EYFP and ECFP into the ROSA26 locus. *BMC Dev. Biol.* 1:4. https://doi.org/10.1186/1471-213X-1-4

Sun, J., A. Ramos, B. Chapman, J.B. Johnnidis, L. Le, Y.J. Ho, A. Klein, O. Hofmann, and F.D. Camargo. 2014. Clonal dynamics of native haematopoiesis. *Nature.* 514:322–327. https://doi.org/10.1038/nature13824

Truong, B.T., Y.J. Lee, T.A. Lodie, D.J. Park, D. Perrotti, N. Watanabe, H.P. Koeffler, H. Nakajima, D.G. Tenen, and S.C. Kogan. 2003. CCAAT/Enhancer binding proteins repress the leukemic phenotype of acute myeloid leukemia. *Blood.* 101:1141–1148. https://doi.org/10.1182/blood-2002-05-1374

Tyner, J.W., C.E. Tognon, D. Bottomly, B. Wilmot, S.E. Kurtz, S.L. Savage, N. Long, A.R. Schultz, E. Traer, M. Abel, et al. 2018. Functional genomic landscape of acute myeloid leukaemia. *Nature.* 562:526–531. https://doi.org/10.1038/s41586-018-0623-z

Ueda, Y., D.W. Cain, M. Kuraoka, M. Kondo, and G. Kelsoe. 2009. IL-1R type I-dependent hemopoietic stem cell proliferation is necessary for inflammatory granulopoiesis and reactive neutrophilia. *J. Immunol.* 182:6477–6484. https://doi.org/10.4049/jimmunol.0803961

van Lochem, E.G., V.H. van der Velden, H.K. Wind, J.G. te Marvelde, N.A. Westerdaal, and J.J. van Dongen. 2004. Immunophenotypic differentiation patterns of normal hematopoiesis in human bone marrow: reference patterns for age-related changes and disease-induced shifts. *Cytometry B Clin. Cytom.* 60B:1–13. https://doi.org/10.1002/cyto.b.20008

Varnum-Finney, B., C. Brashem-Stein, and I.D. Bernstein. 2003. Combined effects of Notch signaling and cytokines induce a multiple log increase in precursors with lymphoid and myeloid reconstituting ability. *Blood.* 101:1784–1789. https://doi.org/10.1182/blood-2002-06-1862

Vas, V., K. Senger, K. Dörr, A. Niebel, and H. Geiger. 2012. Aging of the microenvironment influences clonality in hematopoiesis. *PLoS One.* 7:e42080. https://doi.org/10.1371/journal.pone.0042080

Weisser, M., U.M. Demel, S. Stein, L. Chen-Wichmann, F. Touzot, G. Santilli, S. Sujer, C. Brendel, U. Siler, M. Cavazzana, et al. 2016. Hyperinflammation in patients with chronic granulomatous disease leads to impairment of hematopoietic stem cell functions. *J. Allergy Clin. Immunol.* 138:219–228.e9. https://doi.org/10.1016/j.jaci.2015.11.028

Ye, M., H. Zhang, G. Amabile, H. Yang, P.B. Staber, P. Zhang, E. Levantini, M. Alberich-Jordà, J. Zhang, A. Kawasaki, and D.G. Tenen. 2013. C/EBPa controls acquisition and maintenance of adult haematopoietic stem cell quiescence. *Nat. Cell Biol.* 15:385–394. https://doi.org/10.1038/ncb2698

Yoshihara, H., F. Arai, K. Hosokawa, T. Hagiwara, K. Takubo, Y. Nakamura, Y. Gomei, H. Iwasaki, S. Matsuoka, K. Miyamoto, et al. 2007. Thrombopoietin/MPL signaling regulates hematopoietic stem cell quiescence and interaction with the osteoblastic niche. *Cell Stem Cell.* 1:685–697. https://doi.org/10.1016/j.stem.2007.10.020

Yu, G., L.-G. Wang, Y. Han, and Q.-Y. He. 2012. clusterProfiler: An R package for comparing biological themes among gene clusters. *OMICS.* 16:284–287. https://doi.org/10.1089/omi.2011.0118

Zhang, D.-E., P. Zhang, N.D. Wang, C.J. Hetherington, G.J. Darlington, and D.G. Tenen. 1997. Absence of granulocyte colony-stimulating factor signaling and neutrophil development in CCAAT enhancer binding protein α-deficient mice. *Proc. Natl. Acad. Sci. USA.* 94:569–574. https://doi.org/10.1073/pnas.94.2.569

Zhang, M., F. Liu, P. Zhou, Q. Wang, C. Xu, Y. Li, L. Bian, Y. Liu, J. Zhou, F. Wang, et al. 2019. The MTOR signaling pathway regulates macrophage differentiation from mouse myeloid progenitors by inhibiting autophagy. *Autophagy.* 15:1150–1162. https://doi.org/10.1080/15548627.2019.1578040

Zhang, P., J. Iwasaki-Arai, H. Iwasaki, M.L. Fenyus, T. Dayaram, B.M. Owens, H. Shigematsu, E. Levantini, C.S. Huettner, J.A. Lekstrom-Himes, et al. 2004. Enhancement of hematopoietic stem cell repopulating capacity and self-renewal in the absence of the transcription factor C/EBP alpha. *Immunity.* 21:853–863. https://doi.org/10.1016/j.immuni.2004.11.006

Zheng, R., A.D. Friedman, M. Levis, L. Li, E.G. Weir, and D. Small. 2004. Internal tandem duplication mutation of FLT3 blocks myeloid differentiation through suppression of C/EBPalpha expression. *Blood.* 103:1883–1890. https://doi.org/10.1182/blood-2003-06-1978
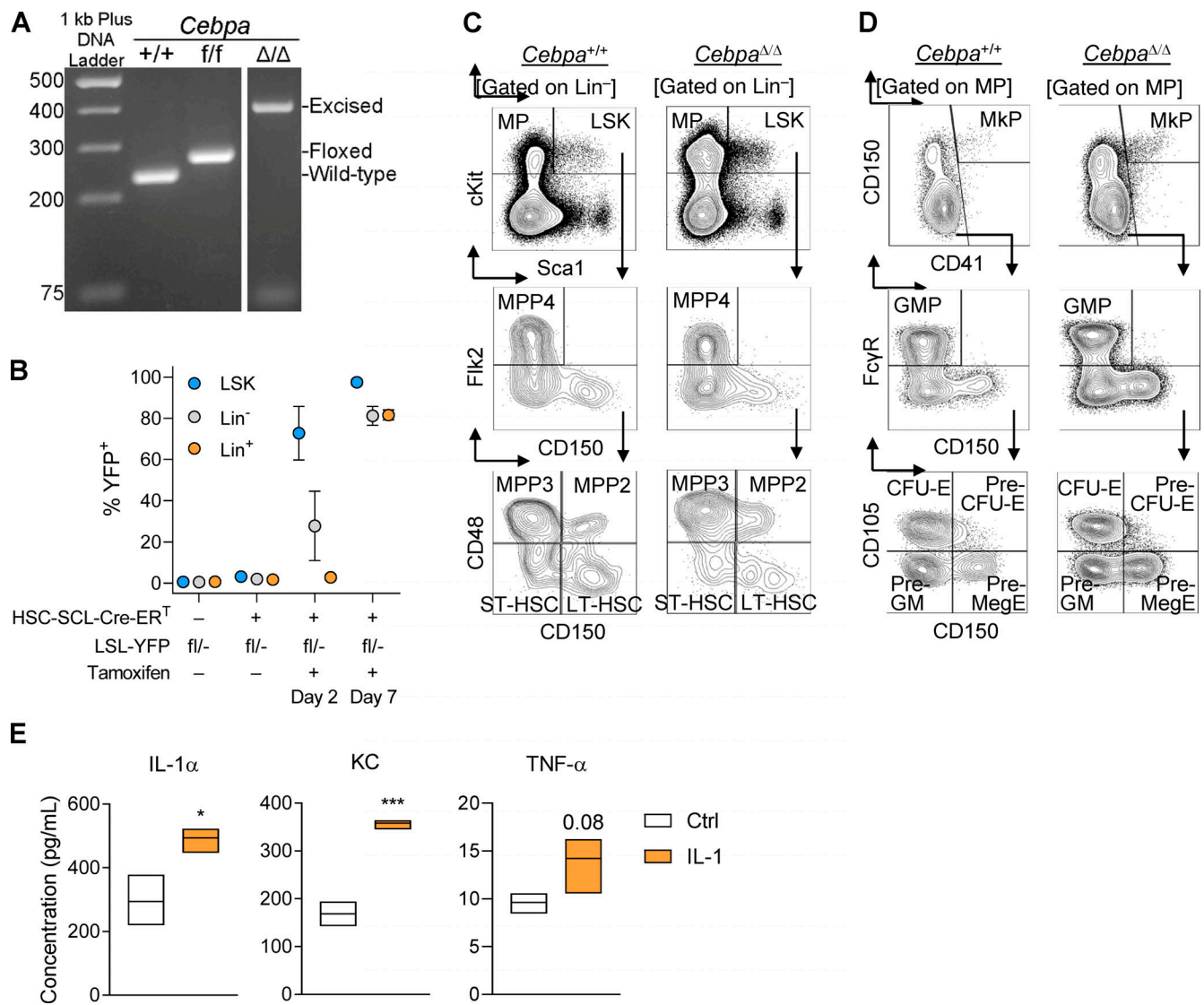
Supplemental material

Figure S1. **Characterization of primary *Cebpa*-knockout mice. (A)** PCR products to detect WT (235-bp), floxed (269-bp), or excised allele (361-bp) run on a 2% agarose gel with 1 kb Plus DNA ladder (Thermo Fisher Scientific). **(B)** Kinetics of tamoxifen-induced YFP expression within Lin⁻Sca1⁺cKit⁺ (LSK), Lin⁻, and Lin⁺ BM fractions. Tamoxifen did not influence HSPC behavior in cell culture or IL-1 levels in BM fluid (data not shown). **(C and D)** Representative flow cytometry plots to characterize HSPC populations (C) and myeloid progenitors (D) from *Cebpa*⁺/⁺ and *Cebpa*^Δ/Δ mice. **(E)** Cytokine analysis of BM fluid from vehicle or chronic IL-1β–treated mice ($n = 3$ mice per group; representative of two experiments). Data are presented as mean ± SD and analyzed by unpaired *t* test (in E). *, $P < 0.05$; ***, $P < 0.001$.
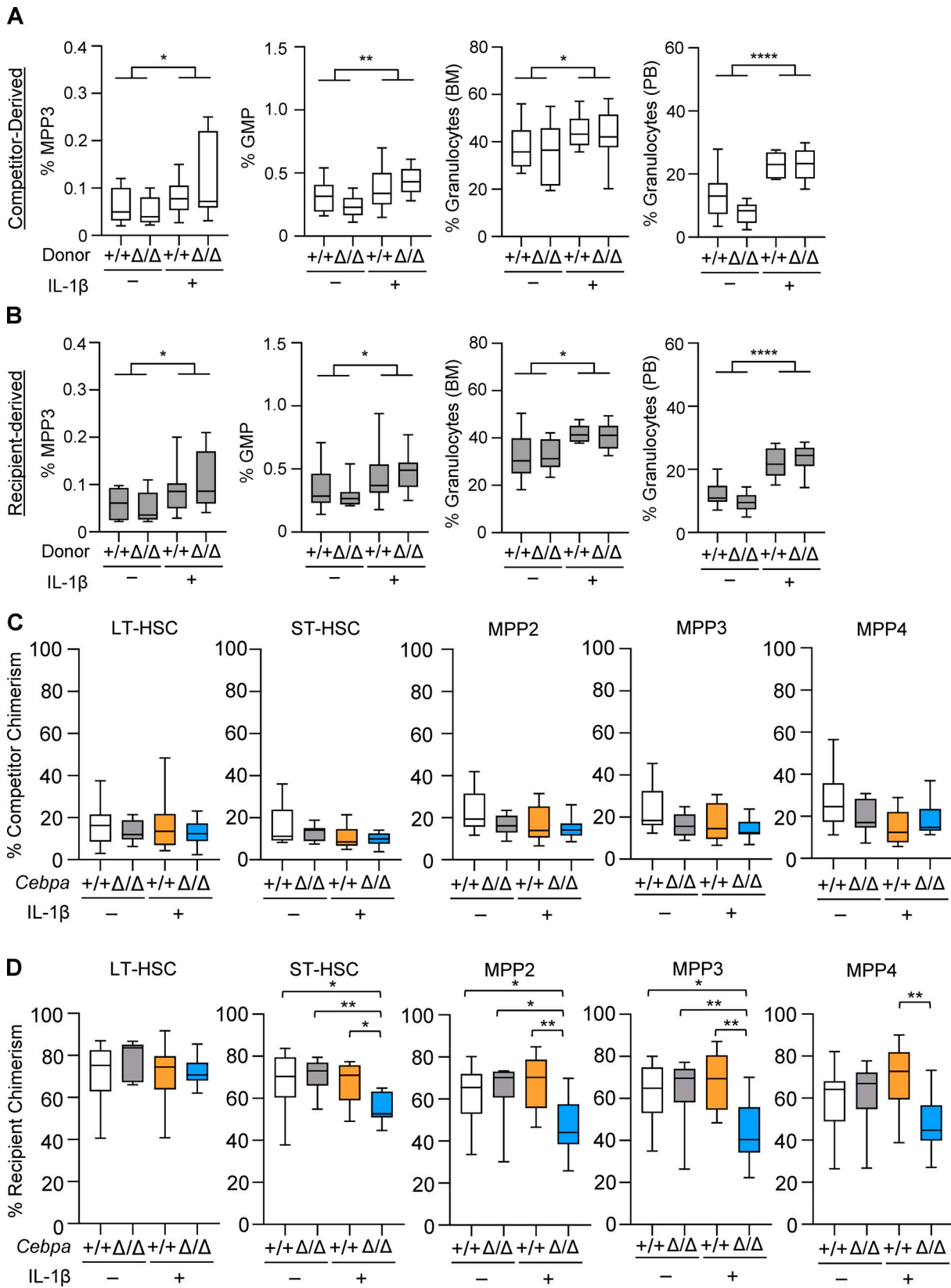
Figure S2. **Myeloid differentiation and chimerism in competitor and recipient HSPCs. (A and B)** Frequency of MPP3, GMP, and granulocytes derived from competitors (A) and recipients (B) in competitive transplants. Graphs in A and B show the percentage of MPP3 within CD45.1⁺ or CD45.2⁺ YFP⁻ cell gates, respectively. PB, peripheral blood. **(C)** Recipient chimerism within indicated HSPC population. **(D)** Competitor chimerism within indicated HSPC population. LT, long-term; ST, short-term. Data are representative of three separate experiments with n = 10 per group, presented as mean ± SD, and analyzed by two-way ANOVA with Tukey's multiple comparisons test. *, $P < 0.05$; **, $P < 0.01$; ****, $P < 0.0001$.
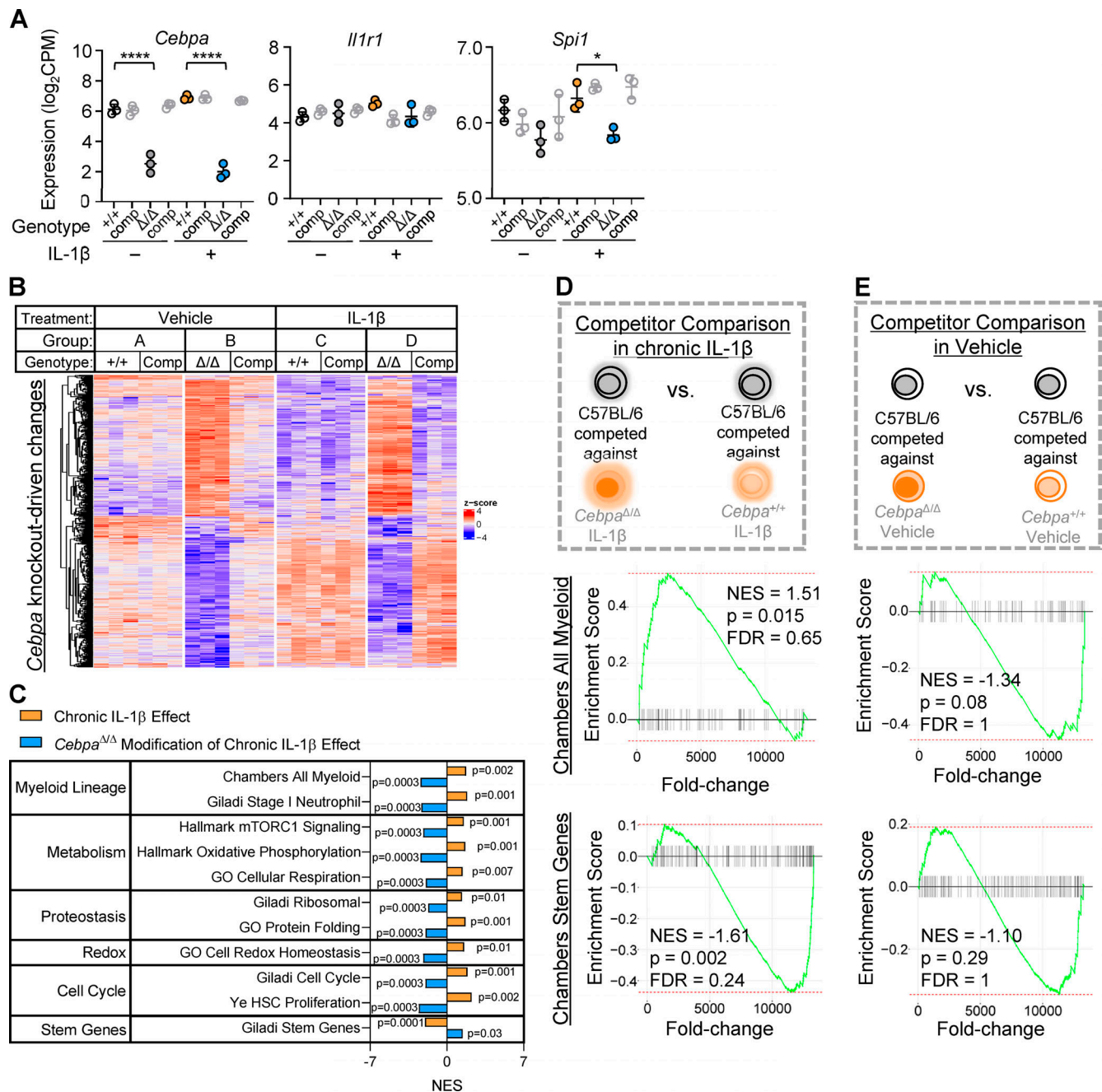
Figure S3. **Cebpa knockout confers a fitness advantage in the context of chronic IL-1β in vivo. (A)** Expression of *Cebpa*, *Il1r1*, and *Spi1* plotted as log$_2$(counts per million) from RNA-seq (*n* = 3 of three to four mice pooled). **(B)** Heatmap of all genes significantly changed (adjusted P < 0.05) by *Cebpa* knockout (genes for heatmap are listed in Table S1). **(C)** Table summarizing the GSEA normalized enrichment score (NES) for select gene sets for "chronic IL-1β effect" and "*Cebpa*$^{Δ/Δ}$ modification of chronic IL-1β effect" pairwise comparisons. **(D and E)** GSEA with "Chambers all myeloid" and "Chambers stem genes" gene sets. **(D)** Schematic and enrichment plots for pairwise comparison between C57BL/6 MPP3 competed against *Cebpa*$^{Δ/Δ}$ or *Cebpa*$^{+/+}$ from chronic IL-1β–treated mice. **(E)** Schematic and enrichment plots for pairwise comparison between C57BL/6 MPP3 competed against *Cebpa*$^{Δ/Δ}$ or *Cebpa*$^{+/+}$ from vehicle-treated mice. FDR, false discovery rate; NES, normalized enrichment score. Data are presented as mean ± SD and analyzed by two-way ANOVA with Tukey's multiple comparisons test (in A). *, P < 0.05; ****, P < 0.0001.
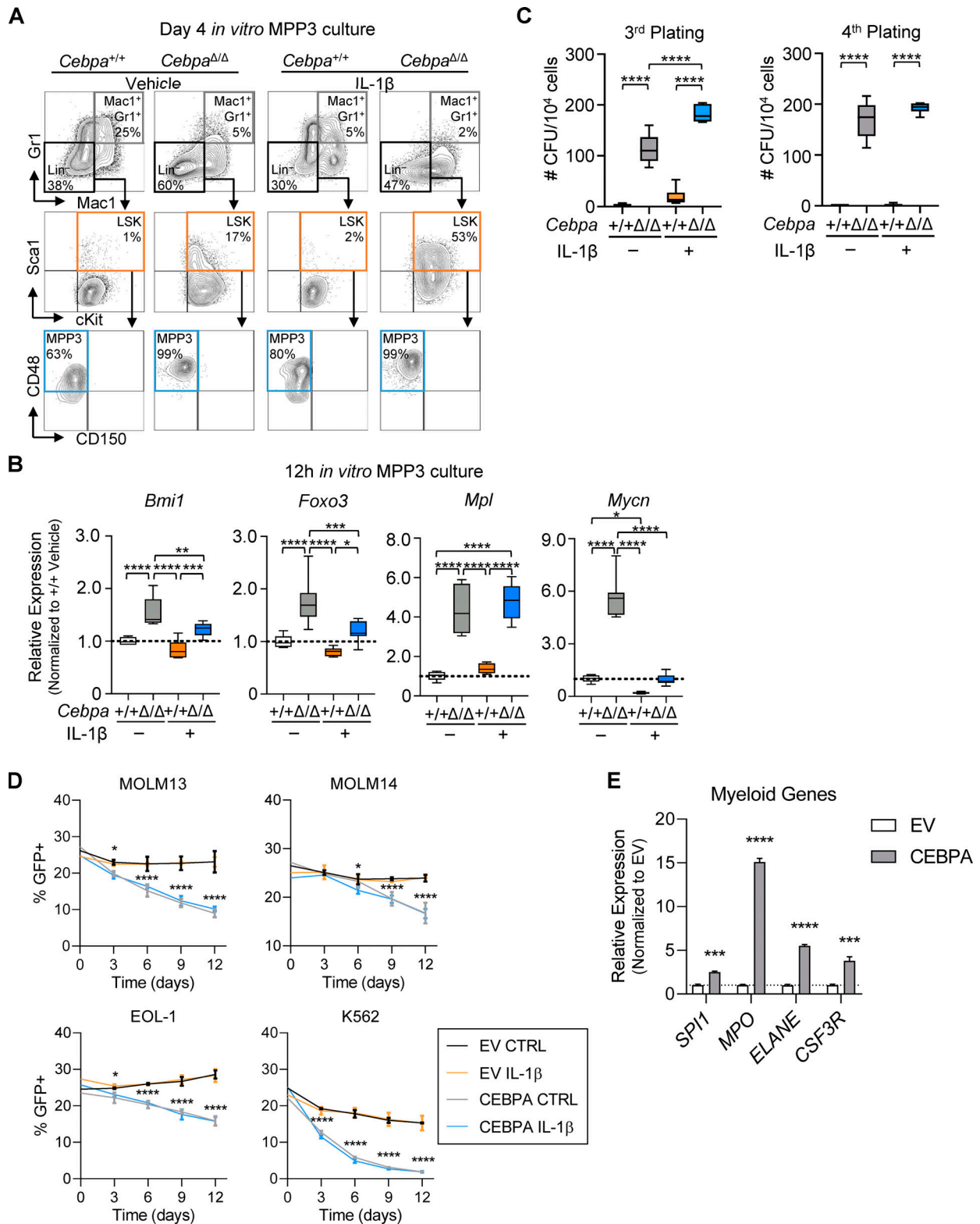
Figure S4. CEBPA regulates expression of self-renewal and myeloid genes and cell competition in culture. (A and B) MPP3 liquid culture (data are representative of two experiments with *n* = 3 per group). **(A)** Representative flow cytometry plots for MPP3 cell culture at day 4. **(B)** Relative expression of self-renewal genes (*Bmi1*, *Foxo3*, *Mpl*, and *Mycn*) calculated by first normalizing to *Gusb* within each group, then normalizing to *Cebpa*$^{+/+}$ vehicle group from MPP3 cell culture at 12 h. **(C)** MPP3 CFU assay (data are representative of two experiments with *n* = 3 or 6 per group): third and fourth plating CFU counts per plate upon replating 10^4 cells. **(D and E)** Cell culture of AML cell lines MOLM-13, MOLM-14, EOL-1, and K562 (representative of two experiments with *n* = 3 per group). **(D)** Cell competition dynamics. **(E)** Gene expression analysis of CEBPA target genes from sorted GFP$^+$ MOLM-13 cells at day 6. EV, empty vector. Data are presented as mean ± SD and analyzed by two-way ANOVA with Tukey's multiple comparisons test (B–D) or unpaired *t* test (E). *, P < 0.05; **, P < 0.01; ***, P < 0.001; ****, P < 0.0001.

Provided online is one table. Table S1 lists gene names from heatmaps in Figs. 5 B, 6 C, 7 C, and S3 B.